

## SECURITY CLASSIFICATION OF THIS PAGE

## REPORT DOCUMENTATION PAGE

1a. REPORT SECURITY CLASSIFICATION Unclassified		1b. RESTRICTIVE MARKINGS													
2a. SECURITY CLASSIFICATION AUTHORITY  2b. DECLASSIFICATION/DOWNGRADING SCHEDULE		3. DISTRIBUTION/AVAILABILITY OF REPORT Unclassified/Unlimited													
4. PERFORMING ORGANIZATION REPORT NUMBER(S) Technical Report #12		5. MONITORING ORGANIZATION REPORT NUMBER(S)													
6a. NAME OF PERFORMING ORGANIZATION University of Minnesota	6b. OFFICE SYMBOL (if applicable)	7a. NAME OF MONITORING ORGANIZATION Office of Naval Research													
6c. ADDRESS (City, State, and Zip Code) Dept. of Chemical Engineering & Materials Science University of Minnesota Minneapolis, MN 55455		7b. ADDRESS (City, State and Zip Code) 800 Quincy Street North Arlington, VA 22217-5000													
8a. NAME OF FUNDING/SPONSORING ORGANIZATION Office of Naval Research	8b. OFFICE SYMBOL (if applicable) ONR	9. PROCUREMENT INSTRUMENT IDENTIFICATION NUMBER Contract No. N/N00014-93-1-0563													
8c. ADDRESS (City, State, and Zip Code) 800 Quincy Street North Arlington, VA 22217-5000		10. SOURCE OF FUNDING NUMBERS PROGRAM ELEMENT NO.      PROJECT NO.      TASK NO.      WORK UNIT ACCESSION NO.													
11. TITLE (Include Security Classification) Epitaxial Interactions Between Molecular Overlays and Ordered Substrates															
12. PERSONAL AUTHOR(S) Andrew C. Hillier and Michael D. Ward															
13a. TYPE OF REPORT Technical	13b. TIME COVERED FROM 5/11/95 TO 6/30/96	14. DATE OF REPORT (Year, Month, Day) 96/5/13	15. PAGE COUNT 26												
16. SUPPLEMENTARY to be published in Phys. Rev. B															
17. COSATI CODES <table border="1"><tr><th>FIELD</th><th>GROUP</th><th>SUB-GROUP</th></tr><tr><td></td><td></td><td></td></tr><tr><td></td><td></td><td></td></tr><tr><td></td><td></td><td></td></tr></table>		FIELD	GROUP	SUB-GROUP										18. SUBJECT TERMS (Continue on reverse if necessary and identify by block number) Organic Conductor, Atomic Force Microscopy, Nucleation, Epitaxy	
FIELD	GROUP	SUB-GROUP													
19. ABSTRACT (CONTINUE ON REVERSE AND IDENTIFY BY BLOCK NUMBER) A framework for evaluating the epitaxy of ordered organic overlays of generic symmetry on ordered substrates is described that combines a computationally efficient method for explicit determination of the type of epitaxy (i.e., commensurism, coincidence, or incommensurism) and overlayer azimuthal orientation with an analysis of the elastic properties of the overlayer and the overlayer-substrate interface. The azimuthal orientations predicted by this function agree with values predicted by semi-empirical potential energy calculations and observed experimentally for previously reported organic overlays which are demonstrated here to be coincident, including electrochemically grown overlays of molecular conductors. Calculations based on this analytical approach are much less computationally intensive than potential energy calculations as the number of computational operations is independent of the overlayer size chosen for analysis. This enables analyses to be performed for the large overlayer basis sets common for molecular overlays. Furthermore, this facilitates the analysis of coincident overlays, for which the overlayer size needs to be large enough to establish the phasing relationship between the substrate and large non-primitive overlays supercell so that the global minimum with respect to azimuthal angle can be determined. The computational efficiency of this method also enables convenient examination of numerous possible reconstructed overlayer configurations in which the lattice parameters are bracketed around those of the native overlayer, thereby allowing examination of possible epitaxy-driven overlayer reconstructions. When combined with calculated intralayer and overlayer-substrate elastic constants this method provides a strategy for the design of heteroepitaxial molecular films.															
20. DISTRIBUTION/AVAILABILITY OF ABSTRACT <input checked="" type="checkbox"/> UNCLASSIFIED/UNLIMITED <input type="checkbox"/> SAME AS RPT <input type="checkbox"/> OTIC USERS		21. ABSTRACT SECURITY CLASSIFICATION Unclassified													
22a. NAME OF RESPONSIBLE INDIVIDUAL Michael D. Ward		22b. TELEPHONE (Include Area Code) (612) 625-3062	22c. OFFICE SYMBOL												

DD FORM 1473, 84 MAR

83 APR edition may be used until exhausted.

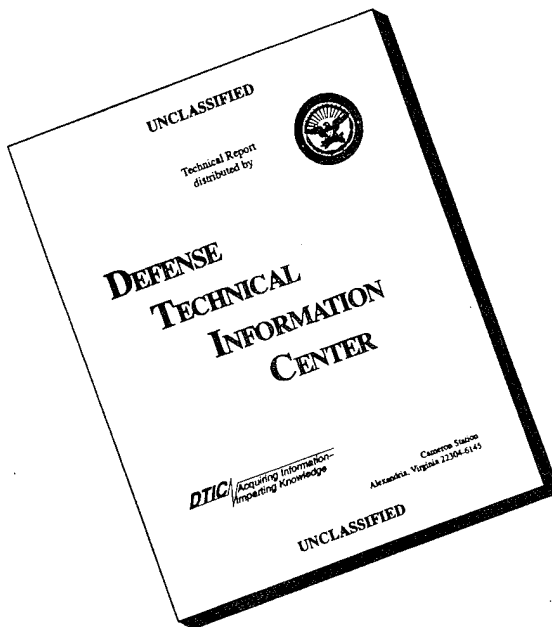
All other editions are obsolete.

SECURITY CLASSIFICATION OF THIS PAGE

Unclassified

19960524  
059

# DISCLAIMER NOTICE



THIS DOCUMENT IS BEST  
QUALITY AVAILABLE. THE  
COPY FURNISHED TO DTIC  
CONTAINED A SIGNIFICANT  
NUMBER OF PAGES WHICH DO  
NOT REPRODUCE LEGIBLY.

**OFFICE OF NAVAL RESEARCH**

Contract N00014-93-1-0563

Technical Report No. 12

"Epitaxial Interactions Between Molecular Overlayers and  
Ordered Substrates"

by

Andrew C. Hillier\* and Michael D. Ward

to be published in

Phys. Rev. B

Department of Chemical Engineering and Materials Science  
University of Minneapolis  
421 Washington Avenue SE  
Minneapolis, MN 55455

May 1996

Reproduction in whole or in part is permitted for  
any purpose of the United States Government.

This document has been approved for public release and sale;  
its distribution is unlimited.

\*Current address: Department of Chemical Engineering, University of Virginia, Charlottesville, VA 22902.

## Epitaxial Interactions Between Molecular Overlayers and Ordered Substrates

Andrew C. Hillier<sup>†</sup> and Michael D. Ward\*

Department of Chemical Engineering and Materials Science, University of Minnesota,  
Amundson Hall, 421 Washington Ave. SE, Minneapolis, MN 55455

### ABSTRACT

A framework for evaluating the epitaxy of ordered organic overayers of generic symmetry on ordered substrates is described that combines a computationally efficient method for explicit determination of the type of epitaxy (i.e., commensurism, coincidence, or incommensurism) and overlayer azimuthal orientation with an analysis of the elastic properties of the overlayer and the overlayer-substrate interface. The azimuthal orientations predicted by this function agree with values predicted by semi-empirical potential energy calculations and observed experimentally for previously reported organic overayers which are demonstrated here to be coincident, including electrochemically grown overayers of molecular conductors. Calculations based on this analytical approach are much less computationally intensive than potential energy calculations as the number of computational operations is independent of the overlayer size chosen for analysis. This enables analyses to be performed for the large overlayer basis sets common for molecular overayers. Furthermore, this facilitates the analysis of coincident overayers, for which the overlayer size needs to be large enough to establish the phasing relationship between the substrate and large non-primitive overlayer supercell so that the global minimum with respect to azimuthal angle can be determined. The computational efficiency of this method also enables convenient examination of numerous possible reconstructed overlayer configurations in which the lattice parameters are bracketed around those of the native overlayer, thereby allowing examination of possible epitaxy-driven overlayer reconstructions. When combined with calculated intralayer and overlayer-substrate elastic constants this method provides a strategy for the design of heteroepitaxial molecular films.

submitted to *Phys. Rev. B*  
version 2.0: May 3, 1995

<sup>†</sup>Current address: Department of Chemical Engineering, University of Virginia, Charlottesville, VA 22902.

PACS 61.16.Ch; 62.20.Dc; 68.55.-a; 81.15.Lm

### INTRODUCTION

The fabrication of molecular thin films with highly ordered, crystalline structures has received considerable attention in attempts to develop materials for molecular based electronic devices, sensors, displays, and logic elements.<sup>1</sup> The interest in molecular films stems primarily from the ability to systematically tailor the electronic and optical properties by judicious choice of molecular constituents. Mono- and multilayers with potentially conducting redox components have been prepared by the attachment of organosulfur and organosilanes to solid surfaces, with functional multilayers built by chemical reactions on these two-dimensional interfaces.<sup>2,3,4</sup> Epitaxial growth of monolayer and multilayer films of redox-active charge transfer salts has been accomplished in solution using electrochemical methods.<sup>5</sup> Thin films of organic dyes on van der Waals substrates such as graphite, MoS<sub>2</sub>, and SnS<sub>2</sub> have been prepared by molecular beam epitaxy methods.<sup>6</sup> Successful fabrication of molecular films with pre-ordained properties hinges on control of several characteristics, including the supramolecular structure of the film, its azimuthal orientation with the respect to the substrate, and the nature and distribution of defects present in the film.

Investigations of the growth of elemental and inorganic thin films,<sup>7</sup> and to a lesser extent molecular films, indicate that film properties can be influenced significantly by interactions between the primary overlayer and the substrate upon which it forms. These interactions commonly are associated with overlayer-substrate epitaxy in which the overlayer and substrate lattices are "in-phase" so that their interatomic potentials are reinforced. However, the actual structure of an overlayer will reflect a competition between the energy lowering achieved by epitaxy and the energetic penalty associated with any reconstruction of the overlayer lattice from its native form that may be required in order to achieve that epitaxy. Consequently, the design of thin films must take into account the relative strengths of intermolecular interactions in the primary overlayer and those between the overlayer and substrate.<sup>8</sup> Controlling these factors is imperative as reconstruction of the primary overlayer from its native form or stress-induced defects can affect the quality of multilayer films and bulk crystals grown from the primary overlayer.

While there have been significant advances in the understanding of the physical and electronic properties of molecular films, there exists a need for paradigms enabling *a priori* design of heteroepitaxial molecular overlayers. We have been employing a strategy for the design of molecular films in which the native structure of a molecular overlayer, considered to be at or near its minimum energy configuration, is surmised from its structure in bulk crystals, which generally consist of layered structures stacked in the third dimension by weak van der Waals interactions.<sup>9,10</sup> The tendency of molecules to assemble in the solid state into two-dimensional layers with strong intralayer bonding (e.g., through hydrogen bonding, charge-transfer, or heteroatom-heteroatom interactions) suggests that layered motifs in bulk crystals are ideal design elements for the fabrication of heteroepitaxial films on appropriately chosen substrates. This strategy must include methodology for identifying the optimum overlayer structure and its epitaxial relationship with a particular substrate, and for evaluating the energetics of the overlayer and the substrate-overlayer interface. Recent reports have described methods for analyzing overlayer-substrate epitaxy which involve calculation of the total potential energy, use of an elliptical potential,<sup>8</sup> or numerical iteration to determine the degree of fit between the overlayer and substrate lattices.<sup>11</sup> However, these methods tend to be computationally intensive when applied to molecular overlayers due to the large basis sets that are required for these systems.

We report herein a simple analytical method for analyzing overlayer-substrate epitaxy that enables rapid determination of optimum epitaxial relationships with respect to overlayer orientation and structure for generic overlayer lattices. This method provides explicit determination of the type of epitaxy, that is, whether the overlayer is commensurate, coincident, or incommensurate. The computational time is independent of overlayer size, which is particularly important in the case of coincident overlayers for which registry with substrates can only be established by large non-primitive supercells. When combined with calculations of overlayer and overlayer-substrate elastic constants for native overlayers whose structures are surmised from either crystal structures, calculations or experimental data, this approach enables rapid analysis of overlayer-substrate systems and a qualitative assessment of the tendency for overlayer reconstruction from its native

form. The method also enables convenient searching for epitaxial relationships between a rigid substrate and many possible reconstructed forms of an overlayer, and suggests that *a priori* design of overlayer-substrate systems is feasible.

## METHODS AND MATERIALS

Molecular overlayers were synthesized from reagent grade materials, with bis(ethylendithiolo)-tetraethylfulvalene (ET), tetraethylfulvalene (TTF), tetracyanoquinodimethane (TCNQ), and pentylene (Pe) obtained from Strem Chemicals, Newburyport, MA. Solvents used for electrodeposited molecular films were HPLC grade. The n-Bu<sub>4</sub>N<sup>+</sup>ClO<sub>4</sub><sup>-</sup> electrolyte was obtained commercially (Aldrich, Milwaukee, WI) and was recrystallized from acetonitrile prior to use. The electrolyte n-Bu<sub>4</sub>N<sup>+</sup>I<sub>3</sub><sup>-</sup> was prepared by a previously reported method<sup>12</sup> in which I<sub>2</sub> were added to a boiling solution of chloroform or water containing excess n-Bu<sub>4</sub>N<sup>+</sup>I<sup>-</sup> (Aldrich, Milwaukee, WI). The black precipitate formed upon mixing was recrystallized twice from methanol to provide dark, lustrous crystals of n-Bu<sub>4</sub>N<sup>+</sup>I<sub>3</sub><sup>-</sup> and the purity was confirmed by elemental analysis. Electrochemical syntheses and *in situ* real-time atomic force microscopy of the (ET)<sub>2</sub>I<sub>3</sub> and Pe<sub>2</sub>(ClO<sub>4</sub>) overlayers were performed in a commercially available fluid cell (Digital Instruments, Santa Barbara, CA) adapted for electrochemical growth, as described previously.<sup>13,14</sup> A three-electrode design was employed for electrochemical measurements with a highly oriented pyrolytic graphite (HOPG) substrate (Union Carbide) serving as the working electrode and Pt counter and reference electrodes placed in the outlet of the fluid cell. The HOPG substrate electrode was cleaved to expose a fresh surface prior to use. Overlays of (ET)<sub>2</sub>I<sub>3</sub> and (Pe)<sub>2</sub>ClO<sub>4</sub> were grown by electrochemical oxidation of ET and Pe, respectively, in acetonitrile containing the respective electrolytes under conditions similar to those previously reported for the electrosynthesis of bulk crystals.<sup>5,15,16</sup> Au(111) substrates for deposition of the (TTF)(TCNQ) overlayers were prepared by melting high purity gold wire (99.999%) in a oxygen/hydrogen flame to expose (111) oriented facets.

Scanning tunneling (STM) and atomic force microscope (AFM) experiments were performed with a Nanoscope III Multimode scanning probe microscope (Digital Instruments, Santa Barbara, CA). STM tips consisted of mechanically cut Pt/Ir wires and AFM probes (Nanoprobe, Park Scientific, Palo Alto, CA) consisted of triangular silicon nitride cantilevers (force constant ~ 0.06 N m<sup>-1</sup>) with integrated pyramidal tips. The AFM was equipped with a scan head having a maximum scan range of 12  $\mu\text{m}$  by 12  $\mu\text{m}$ , while the STM employed a scanner with maximum range of 5  $\mu\text{m}$  by 5  $\mu\text{m}$ . AFM images were acquired in the contact mode under constant force conditions, with integral and proportional gains of 4.0 and 7.0, respectively. The tip-sample force was minimized before imaging by reducing the set point to a value just below tip disengagement. The azimuthal orientations of the (ET)<sub>2</sub>I<sub>3</sub> and Pe<sub>2</sub>(ClO<sub>4</sub>) overlayers with respect to the HOPG substrate were determined by imaging an exposed region of the substrate immediately before or after imaging of the overlayer, or by imaging the substrate lattice underneath the overlayer after removing the overlayer mechanically by increasing the force exerted by the AFM tip.

Potential energy calculations for the overlayer-substrate interfaces were performed on a Hewlett-Packard 710 workstation with a Universal Force Field<sup>7</sup> based on a Lennard-Jones 6-12 potential function integrated with a customized Fortran code that allowed approach, translation, and rotation of a overlayer-substrate molecular interface. Energy minimized overlayer structures and intralayer potentials were calculated using the Cerius molecular modeling program (Molecular Simulations, version) and the Universal Force Field. Electrostatic interactions were neglected in these calculations as it was determined that the results were rather insensitive to these contributions owing to their long range nature. The native structures of the overlayers were surmised from layered motifs in bulk crystals whose structures were obtained from the Cambridge Structural Database (version 2.3.7). These native structures served as the initial trials in energy minimization and intralayer potential calculations. Stress and elastic constants were calculated directly from the calculated potentials. Structural models were visualized with the Computer Assisted Chemistry (CAChe, Inc.) molecular modeling program. Calculations of interface misfit and epitaxy using the analytical function described here were performed on either the 710 workstation, or on a IBM 486

personal computer using a program written in our laboratory (EpiCalc<sup>©</sup>), which runs in the Windows™ v. 3.1 environment. EpiCalc<sup>©</sup> is available on the World Wide Web at <http://www.cens.umn.edu/research/ward>.

## RESULTS AND DISCUSSION

The spatial configuration of a molecule or assembly of molecules at an interface is determined by a minimum in the total system energy. The potential energy of an atom B residing near a substrate plane of atoms A, assuming strict additivity of interaction energies between neighboring atoms, is the sum of interactions between atom B and the individual atoms in layer A.<sup>18</sup> If atom B belongs to a semi-infinite layer the total potential energy of the entire system can be described by eq. (1), where  $r^A$  and  $r^B$  represent the positions of the atoms in layers A and B, respectively, and last two terms represent the self-energies of the substrate and overlayer, respectively.

$$V_T(r) = \sum_i \sum_j V_{ij}(r_i^A - r_j^A) + \frac{1}{2} \sum_{i,j} V_{ii}(r_i^A - r_i^A) + \frac{1}{2} \sum_{i,i} V_{BB}(r_i^B - r_i^B) \quad (1)$$

The optimum overlayer-substrate configuration can be determined by minimizing  $V_T(r)$  with respect to the structure of the overlayer, and its separation, position, and azimuthal orientation with respect to the substrate. Such computations can be daunting due to the large number of possible overlayer-substrate configurations. Furthermore, the total system energy is not a strictly convex function, which makes determination of the global minimum configuration difficult and mathematically uncertain. This problem can be simplified somewhat by assuming a constant substrate potential  $V_{AA}$ , which generally will be valid for "rigid" substrates whose structure is unaffected by the presence of the overlayer. This allows reduction of eq. (1) to a form including only  $V_{AB}$  and  $V_{BB}$ . The relative magnitudes of these potentials will dictate whether the overlayer retains its native form ( $V_{BB} > V_{AB}$ ) or is reconstructed ( $V_{AB} > V_{BB}$ ). Additionally,  $V_T$  will be decreased when epitaxy reinforces attractive interactions between the overlayer and substrate.

**The Epitaxial Interface.** Epitaxy generally is used to describe lattice registry, or equivalently the degree of "phase matching", between two opposing lattice planes (although it was originally used to describe the growth of material B on substrate A, with B adopting the structure of A). In simple atomic systems, the criterion used to describe the extent of epitaxy along a specified crystallographic direction is the lattice misfit  $f = (b - a)/a$ , where  $a$  and  $b$  are lattice constants of the substrate and overlayer, respectively.<sup>19</sup> The misfit  $f$  is a one-dimensional parameter and can be used only for two-dimensional systems when the two lattices are of equivalent symmetry and size. Therefore, an alternative approach is required for generic two-dimensional interfaces.

A two-dimensional interface consisting of substrate A and overlayer B can be described by seven parameters (Figure 1). The substrate can be described by lattice constants  $a_1$ ,  $a_2$  and angle  $\alpha$ , the overlayer by  $b_1$ ,  $b_2$  and angle  $\beta$ , and the azimuthal orientation can be defined by the angle  $\theta$  between  $a_1$  and  $b_1$ . The azimuthal relationship between substrate A and overlayer B can be described by a transformation matrix C which relates  $b_1$  and  $b_2$  to  $a_1$  and  $a_2$ , where C is a  $2 \times 2$  matrix with elements  $p_x$ ,  $q_y$ ,  $q_x$ , and  $p_y$  (eq. 2). The values of the matrix elements depend upon the substrate lattice constants, the overlayer lattice constants, and  $\theta$  according to eqs. (3) - (6).

[Figure 1]

$$\begin{bmatrix} b_1 \\ b_2 \end{bmatrix} = [C] \begin{bmatrix} a_1 \\ a_2 \end{bmatrix} = \begin{bmatrix} p_x & q_y \\ q_x & p_y \end{bmatrix} \begin{bmatrix} a_1 \\ a_2 \end{bmatrix} \quad (2)$$

$$p_x = b_1 \sin(\alpha - \theta) / a_1 \sin(\alpha) \quad (3)$$

$$q_y = b_1 \sin(\theta) / a_2 \sin(\alpha) \quad (4)$$

$$q_x = b_2 \sin(\alpha - \theta - \beta) / a_1 \sin(\alpha) \quad (5)$$

$$p_y = b_2 \sin(\theta + \beta) / a_2 \sin(\alpha) \quad (6)$$

The primary value of the transformation matrix is that it describes the interface in convenient terms. The determinant of C is equivalent to the ratio of overlayer to substrate unit cell areas and its value defines whether the system is commensurate, coincident, or incommensurate. However, this determinant does not provide the energetics of the interface. Because the coincidence condition is not as well recognized as the other two and is the main tenet of the following discussion, these conditions are defined here in the context of the properties of this matrix.

**Commensurism:** This condition exists when every overlayer lattice site resides on a particular set of substrate lattice sites. Under this condition  $\det(C)$  and each of the matrix elements assume integral values. Consequently, the overlayer unit cell can be described by a minimum integral number of substrate unit cells at some rotation angle.

**Coincidence:** This condition exists when overlayer sites are coincident with uniformly spaced rows of substrate sites corresponding to a specific lattice direction, such that one of the reciprocal lattice vectors of the overlayer has the same direction and magnitude as the reciprocal lattice vector defining the substrate rows. All the overlayer sites do not reside on substrate sites within these rows. Consequently, there exists a phase mismatch along only one substrate reciprocal lattice vector and the degree of epitaxy is weaker than in a commensurate structure. Under this condition,  $\det(C)$  will be a rational fraction in which both numerator and denominator have integral values.

Coincidence further requires that certain combinations of the matrix coefficients assume integral values at the rotation angle  $\theta$ . In the case of a generic lattice,  $p_x$  and  $q_y$ , or  $p_y$  and  $q_x$ , must be integers. Integral values for these combinations and the set  $p_x+q_y$  and  $q_x+p_y$  are required for coincidence on hexagonal substrates. In both cases, the remaining coefficients must be rational in order for  $\det(C)$  to be a rational fraction. Coincidence implies the existence of a non-primitive overlayer supercell, constructed from an integral number of overlayer unit cells, whose perimeter is commensurate with the substrate. This is equivalent to stating that a coincident overlayer has some overlayer positions (most commonly chosen to be the vertices of the supercell) which are commensurate with substrate sites, while other molecules contained within the supercell are locally

non-commensurate. The degree of epitaxy improves as the number of primitive overlayer cells comprising the non-primitive supercell decreases, as this leads to fewer non-commensurate overlayer sites. Real molecular overlayers will involve a large number of molecules assembled into two-dimensional lattices. The size and symmetry of these lattices will differ substantially from those of typical substrates, arguing against commensurate lattices in the absence of overlayer reconstruction. Consequently, any analysis of overlayer-substrate interfaces must consider the possibility of coincident overlayers.

**Incommensurism:** This condition exists when the overlayer is neither commensurate nor coincident with the substrate.

Two methods have been employed recently to evaluate epitaxy of molecular overlayers, specifically by examining the "degree of epitaxy" for continuously changing values of  $\theta$ . The most complete method involves determination of non-bonded potential energy interactions summed over the entire overlayer-substrate interface. For a particular overlayer orientation and a fixed structure (in which the overlayer and substrate are considered to be rigid so that  $V_{AA}$  and  $V_{BB}$  are constant), the interface potential can be described by eq. (7), that is, by summation of the individual molecule-substrate potentials  $V_{AB}$  where  $i$  and  $j$  refer to the summation over the substrate A and overlayer B atoms. The interaction potential  $V_{AB}$  can include van der Waals attraction, electron-core repulsion, electrostatic interactions and hydrogen bonding, which are generally weaker than covalent forces and are assumed to be pairwise additive such that the interaction between numerous atoms or molecules can be determined with a simple sum of individual atom pair interactions using any one of several accepted empirical and semi-empirical potential force fields.<sup>20,21,22,23</sup> It can be surmised from eq. (7) that  $V_T$  will depend upon the azimuthal angle  $\theta$ , with a global minimum in  $V_T$  at a value of  $\theta$  at which epitaxy is maximized. However, for an overlayer and substrate, each having  $n \times n$  atoms, the potential method requires  $n^4$  calculations at each value of  $\theta$  examined. This becomes prohibitive for computations involving

large unit cells or large overayers consisting of multiple unit cells. Furthermore, the semi-empirical nature of these calculations does not guarantee accuracy.

$$V_T(r) = \sum_i \sum_j V_{AB}(r_i^*, r_j^*) \quad (7)$$

An alternative method for determining the influence of periodic interfacial interactions at a two-dimensional interface has been reported in which the local misfits  $f$  between individual atomic or molecular sites in the overlayer and substrate are summed over the entire interface.<sup>11</sup> The summation can be described by the two-dimensional misfit parameter  $D(\theta)$  in eq. (8), where  $a_1$  and  $a_2$  represent the substrate lattice dimensions and C is the transformation matrix relating overlayer point, with matrix coefficients  $[C]$  and indexed by integers  $i$  and  $j$ , to the nearest substrate lattice point, given by  $\text{int}[C]$ . This is a discrete two-dimensional misfit calculation in which the energy units are arbitrary, and the value of  $\theta$  at which  $D(\theta)$  is minimum signifies the azimuthal angle at which epitaxy is maximized. If the system is coincident one vector component of the misfit will disappear and the depth of the minimum will depend upon the sum of misfit, reaching a maximum value for incommensurate overayers. This method is conceptually simple and retains the essential features of the complete potential energy calculation given in Eq. (7), and requires only  $n^2$  calculations per configuration. However, it suffers from being a numerical method rather than an analytical one, has little direct theoretical significance, and remains computationally intensive if many overlayer cell structures and orientations are to be analyzed.

$$D(\theta) = \sum_i \sum_j (i - j) \cdot \{[C] - \text{int}[C]\} \cdot \begin{pmatrix} a_1 \\ a_2 \end{pmatrix} \quad (8)$$

**An analytical approach to epitaxy characterization.** The computational intensiveness of these methods prompted us to develop an analytical method for evaluating epitaxy for overlayer-substrate systems. This method, which is based on an extension of earlier treatments for simple

one and two-dimensional lattices,<sup>24,25</sup> relies on a dimensionless potential energy  $V/V_0$ , which for one-dimensional lattice can be described by eq. (9), where  $a$  represents the lattice periodicity.

$$\frac{V(x)}{V_0} = \cos\left(\frac{2\pi}{a}x\right) \quad (9)$$

The interaction between a substrate lattice and an overlayer lattice is governed by the overlap of their potential energy surfaces, with these interactions reinforced when the lattices are "in-phase." The potential of a rigid one-dimensional overlayer-substrate interface can be described by eq. (10), and for an overlayer with unit cell dimension  $b$ , the coordinates of atom  $i$  are given by eq. (11). Substituting eq. (11) into Eq. (10) gives eq. (12), which describes the potential of the one-dimensional interface at different values of  $x$ . This can be expressed in the mathematically equivalent form of eq. (13) by replacing the summation by an integral and defining the mismatch between the lattice periods  $a$  and  $b$  by the lattice misfit  $f = (b-a)/a$ . The expression in eq. (13) is a dimensionless potential which describes the "degree of commensurability" between two one-dimensional lattices with respect to the misfit  $f$ , where  $M$  is a whole number corresponding to the multiples of lattice  $b$ . Under conditions where the lattice period  $a$  is equal to  $b$  ( $f = 0$ ) the dimensionless potential achieves a minimum at  $V/V_0 = 0$ . As  $f$  increases,  $V/V_0$  actually increases through a maximum at  $f = 0.04$  before decreasing again in an oscillatory fashion. At large misfit,  $V/V_0$  reaches a constant value of one. Eq. 13 provides an analytical expression which can be used to establish the overlayer-substrate configuration at which  $V/V_0$  is minimized, that is, at a configuration representing the best match between the two lattices.

$$\frac{V(x)}{V_0} = \left[ 1 - \cos\left(\frac{2\pi}{a}x\right) \right] \quad (10)$$

$$\frac{V}{V_0} = (2M+1) - \frac{\sin[(2M+1)\pi(f+1)]}{\sin[\pi(f+1)]} \quad (11)$$

This method can be extended to generic two-dimensional overlayer-substrate interfaces by adopting a previously reported approach which addressed trivial two-dimensional lattices. The potential of a two-dimensional periodic lattice can be described by eq. (14), and for an overlayer with unit cell dimensions  $b_x$  and  $b_y$  the coordinates of atoms  $i$  and  $j$  are given by eqs. (15) and (16). Substituting eqs. (15) and (16) into eqn. (14) provides the dimensionless potential in eq. (17), in which the summation again can be replaced by an integral to give the analytical function in eq. (18).

$$\frac{V(x)}{V_0} = \frac{1}{2} [2 - \cos(2\pi x) - \cos(2\pi y)] \quad (14)$$

$$x_i = (i-j) \cdot [C] \cdot \begin{pmatrix} 1 \\ 0 \end{pmatrix} \quad i = -M, \dots, M \quad (15)$$

$$y_j = (i-j) \cdot [C] \cdot \begin{pmatrix} 0 \\ 1 \end{pmatrix} \quad j = -N, \dots, N \quad (16)$$

$$\frac{V}{V_0} = \sum_i \sum_j \left\{ 2 - \cos \left[ 2\pi(i-j) \cdot [C] \cdot \begin{pmatrix} 1 \\ 0 \end{pmatrix} \right] - \cos \left[ 2\pi(i-j) \cdot [C] \cdot \begin{pmatrix} 0 \\ 1 \end{pmatrix} \right] \right\} \quad (17)$$

$$\frac{V}{V_0} = \frac{1}{2} \left[ 2(2M+1)(2N+1) - \frac{\sin[(2M+1)\pi q_x] \sin[(2N+1)\pi q_y]}{\sin[\pi q_x] \sin[\pi q_y]} \right] \quad (18)$$

$$x_i = ib \quad i = 0, \pm 1, \dots, \pm M$$

$$\frac{\sin[(2M+1)\pi q_x] \sin[(2N+1)\pi q_y]}{\sin[\pi q_x] \sin[\pi q_y]} \left\{ \frac{\sin[(2N+1)\pi p_y]}{\sin[\pi p_y]} \right\}$$

The potential  $V/V_0$  can be calculated for orientations defined by the component of matrix  $C$  for an overlayer with  $M \times N$  unit cells. This potential assumes discrete values which depend upon the type of epitaxy, with commensurism, coincidence, and incommensurism resulting in values of 0, 1/2 and 1, respectively. Notably, the computational requirements for determining misfit with eq. (18) are minimal as a calculation at a particular value of  $\theta$  requires only one operation and is independent of overlayer size, in contrast to the aforementioned methods. The validity of this approach can be illustrated by comparing the azimuthal orientation of model systems with that predicted from of eq (18). For a substrate having lattice constants  $a_1 = a_2$  contacted by a  $20 \times 20$  overlayer of identical symmetry but with lattice constants of  $b_1 = b_2 = 2a_1$ ,  $V/V_0$  passes through a minimum at  $V/V_0 = 0$  at  $\theta = 0^\circ$  and  $\theta = 90^\circ$ , as surmised by visual inspection of these lattices (Figure 2). The value of  $\det(C) = 4$  for this commensurate overlayer is identical to the 4:1 ratio of unit cell areas. As the azimuthal angle of the overlayer departs from the commensurate orientation,  $V/V_0$  increases in an oscillatory manner due to the increasing misfit. Regions of incommensurism are signified by a value of  $V/V_0 = 1$ . The coincident condition can be illustrated by a substrate having lattice constants  $a_1 = a_2$  and an overlayer of different symmetry with lattice constants of  $b_1 = 1.6a_1$ ,  $b_2 = 1.8a_2$  and  $\beta = 146.25^\circ$ . Overlayer lattice points along  $b_1$  are coincident with lattice vector  $a_1$ , and the reciprocal lattice vectors  $a_1^*$  and  $b_1^*$  are identical. Calculation of  $V/V_0$  predicts the presence of coincidence at  $\theta = 0^\circ$  and  $90^\circ$ , as surmised by visual inspection of these lattices. This overlayer is described by a  $5 \times 2$  non-primitive supercell whose vertices are commensurate with the substrate.

differs somewhat from the other two functions due to its discrete and linear nature. This data indicates that the dependence of  $V_T$  on  $\theta$  is exactly reproduced with  $V/V_0$  for this overlayer-substrate interface. Actual molecular overlayers are likely to exhibit differences in  $V_T$  and  $V/V_0$  as  $V/V_0$  does not account for local molecule-substrate interactions. However, as the overlayer size is increased these local contributions will become increasingly dominated by the in-phase components defined by the commensurate non-primitive supercell so that only the periodic terms remain and the forms of  $V_T$  and  $V/V_0$  converge to the same global minimum. This can be illustrated by examining an interface comprising a substrate with  $a_1 = a_2 = 2.46 \text{ \AA}$  and  $\alpha = 60^\circ$  (graphite) having three atoms per unit cell and an overlayer with  $b_1 = 6.61 \text{ \AA}$ ,  $b_2 = 9.1 \text{ \AA}$ , and  $\beta = 110^\circ$  having three atoms (molecules) per unit cell (this particular overlayer corresponds to one that mimicks the triiodide layer in the (001) plane of  $\beta(\text{Et}_2\text{I}_3)$ , which is described below). Differences in form and minima are evident for a  $3 \times 3$  overlayer. However, the two functions progressively converge to the same form upon increasing overlayer size ( $5 \times 5$  and  $7 \times 7$ ), eventually exhibiting identical minima at  $\theta = 190^\circ$  where the value of  $V/V_0 = 0.5$  indicates coincident epitaxy (Figure 4). Therefore,  $V/V_0$  is identical in form to the purely periodic components of  $V_T$  in the limit of increasingly larger overlayer sizes. This illustrates that calculations performed with any of these methods must include a sufficient number of overlayer unit cells in order to establish accurately the phase relationship between the substrate and the commensurate supercell.

[Figure 3]

[Figure 4]

[Figure 2]

The validity of using  $V/V_0$  to evaluate epitaxy can be demonstrated further by comparing the azimuthal angles observed experimentally for several overlayer-substrate systems to those calculated from  $V/V_0$  using the known lattice parameters (Table 1). In nearly every example in Table 1, the orientation of the overlayer predicted by  $V/V_0$  corresponds to that determined experimentally. Particularly interesting are the six polymorphs of perylene-tetracarboxylic

dianhydride (PTCDA) overlayers, for which all but one are epitaxial by coincidence based on V/V<sub>o</sub>. Figures 5 and 6 illustrates the orientation of the lattices identified for selected overlayer-substrate systems from Table 1 and their corresponding V/V<sub>o</sub> dependences on  $\theta$ .

[Table 1]

[Figure 5]  
[Figure 6]

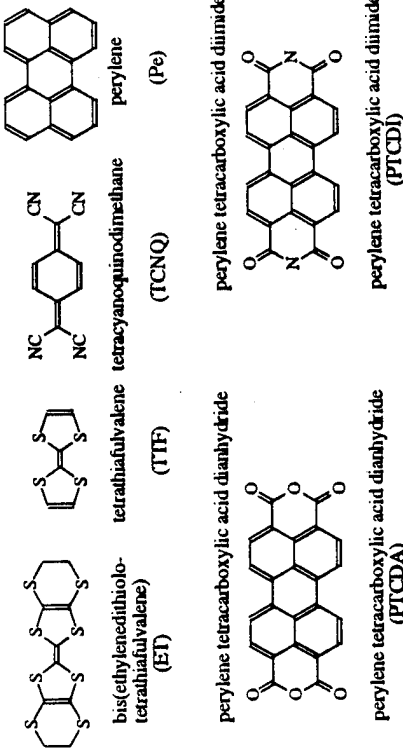


Table 1. Comparison of the experimentally measured and calculated azimuthal angles ( $\theta_{\text{exp}}$  and  $\theta_{\text{cal}}$ , respectively) for various overlayer-substrate systems with overlayer lattice constants  $b_1$ ,  $b_2$  and  $\beta$ .

Organic Overlayer	Substrate <sup>a</sup>	$b_1$ (Å)	$b_2$ (Å)	$\beta$ (deg)	$\theta_{\text{exp}}$ (deg)	$\theta_{\text{cal}}$ (deg)	supercell size <sup>d</sup>	method	ref
PTCDA	MoS <sub>2</sub> <sup>g</sup>	12.4	19.7	88.8	12.7	12.7	3 x 1	STM	26
	HOPG <sup>g</sup>	15.2	21.6	90.0	13	11.3	3 x 3	STM	8a, 27
	HOPG <sup>g</sup>	15.7	20.0	90.0	19	18.6	3 x 2	Theor	8a, 27
	HOPG <sup>g</sup>	12.7	19.2	89.5	3.1	3.2	3 x 1	STM	11
	HOPG <sup>g</sup>	12.4	19.4	90.0	9.9	19.9	2 x 1	STM	11
	HOPG <sup>g</sup>	12.0	20.2	90.0	2.5	12.3	3 x 3	LEED	28
PTCDI	HOPG <sup>g</sup>	12.5	19.1	90.0	3.0	b	-	LEED	28
	HOPG <sup>g</sup>	12.7	19.2	89.5	3.2	3.2	3 x 1	STM	28
	Cu(100) <sup>f</sup>	14.5	18.1	90.0	45	45	1 x 1	LEED	29
	HOPG <sup>g</sup>	14.5	16.9	83.6	12.7	12.7	2 x 2	STM	23
	MoS <sub>2</sub> <sup>g</sup>	14.5	17.2	83.1	10.9	10.8	1 x 3	STM	23
	MoS <sub>2</sub> <sup>f</sup>	13.7	14.2	90.0	30	30	2 x 2	STM	30
C <sub>60</sub> Pt	Cu(100) <sup>f</sup>	13.8	19.0	96.6	23.4	22.2	1 x 1	LEED	29
	Cu(111) <sup>g</sup>	12.6	12.6	85.0	8	0.35	1 x 3	LEED	31
	Cu(100) <sup>f</sup>	13.7	13.7	90.0	22.5	21.8	1 x 1	LEED	31
	Cu(111) <sup>g</sup>	12.0	12.0	82.0	11	b	-	LEED	31
	Cu(100) <sup>f</sup>	13.7	13.7	90.0	22.5	21.8	1 x 1	LEED	31
	Cu(111) <sup>g</sup>	13.3	13.3	81.5	10.25	11.1	3 x 1	LEED	31
FePt	HOPG <sup>g</sup>	10.9	18.1	87.0	15	9	5 x 2	AFM	32
	(TTF) <sub>2</sub> ClO <sub>4</sub>	11.0	16.5	104.0	c	27	5 x 4	STM	33
	(TTF)(TCNQ)	6.6	9.1	110.0	18	19	1 x 3	AFM	34
	$\beta$ -(ET) <sub>2</sub> Li <sup>e</sup>	7.2	17.3	83.0	15	17	3 x 5	AFM	35
	$\beta$ -(ET) <sub>2</sub> Li <sup>f</sup>								

<sup>a</sup> Lattice constants for substrates: HOPG ( $a_1 = a_2 = 2.46 \text{ \AA} / \alpha = 60^\circ$ ), MoS<sub>2</sub> ( $a_1 = a_2 = 3.16 \text{ \AA} / \alpha = 60^\circ$ ), Cu(100) ( $a_1 = a_2 = 2.56 \text{ \AA} / \alpha = 90^\circ$ ); Cu(111) ( $a_1 = a_2 = 2.36 \text{ \AA} / \alpha = 60^\circ$ ); Au(111) ( $a_1 = a_2 = 2.88 \text{ \AA} / \alpha = 60^\circ$ , bicommonstrate,  $\theta_{\text{exp}}$  was not determined due to experimental difficulties). <sup>d</sup> M and N refer to the multiples of  $b_1$  and  $b_2$  describing the supercell. <sup>e</sup> Lattice parameters given correspond to those of the (001) plane of bulk  $(\text{ET})_{23}$ , which are identical to the lattice constants of the overlayer observed by AFM, within experimental error bulk crystal. <sup>f</sup> Coincident.

These comparisons demonstrate that a simple dimensionless potential  $V/V_o$  can be used to analyze and predict the registry of overlayer-ex-substrate combinations, enabling determination of the type of epitaxy and optimum azimuthal orientation for a particular overlayer structure. The computational time required for this analysis is independent of overlayer size, which is particularly important for analyzing molecular films with large, low-symmetry, oblique unit cells containing large numbers of basis atoms. The dependence of  $V_T$  and  $V/V_o$  on overlayer size depicted in Figure 4 illustrates that calculations performed on coincident overlayers, either with the total potential or  $V/V_o$ , can exhibit shallow and multiple potential minima if the overlayer sizes are

large numbers of basis atoms. The dependence of  $V_T$  and  $V/V_o$  on overlayer size depicted in Figure 4 illustrates that calculations performed on coincident overlayers, either with the total potential or  $V/V_o$ , can exhibit shallow and multiple potential minima if the overlayer sizes are

small. The emergence of a clear global minimum associated with coincident overayers for large overlayer sizes demonstrates that multiple minima or shallow potential functions observed for small overlayer sizes does not necessarily signify incommensurism. The concept of "quasiepitaxy," a condition surmised from apparent lack of commensurism, was advanced recently to explain the formation of low-defect molecular overayers.<sup>3</sup> However, evaluation of  $V/V_0$  for several overayers (Table 1) reveals that most of these are actually coincident, with clearly defined minima at the azimuthal angles indicated. The existence of coincidence does not detract from the ability to form stress-free, low-defect molecular overayers. Indeed, the ability of overayers to be stabilized by coincidence in their essentially unreconstructed is an ideal condition for the formation of high-quality crystalline multilayers and bulk materials grown from these primary overayers.

The computational efficiency of this analytical function also enables systematic searching, within a reasonable time, for reconstructed overayers whose lattice parameters  $b_1$ ,  $b_2$  and  $\beta$  bracketed around the native overayer values so that possible epitaxy-driven reconstructions can be examined. This is performed with a custom-made program, developed in our laboratory, operating in the Windows<sup>TM</sup> environment, which calculates  $V/V_0$  over the full range of  $\theta$  for numerous sets of lattice parameters. Computations performed on a standard 486 processor enable  $>1000$  possible reconstructed forms to be searched and fully analyzed in one hour. However,  $V/V_0$  does not provide the actual overlayer-substrate interaction energy or stability ranking of different epitaxial overlayer-substrate combinations. Rather, its utility lies in narrowing the choice of possible configurations available to a particular overlayer-substrate system.

**Energetics of the overlayer-substrate interface.** Table 1 lists organic overayers that are either commensurate or coincident. The existence of either of these conditions is a reflection of the balance between overlayer-substrate interactions and intermolecular interactions within the layer (intralayer interactions).<sup>36</sup> In the absence of substrate contributions, the overlayer structure will be defined by the global minimum in its potential energy corresponding to a packing motif with high packing density and optimum intermolecular interactions. In contrast, overlayer-substrate

interactions will be maximized by formation of a commensurate overlayer, or to a lesser extent by coincidence, as the phasing of the potential functions is optimized under these conditions. Intralayer forces favor retention of the native form of the overlayer while overlayer-substrate forces at the interface promote reconstruction of the overlayer in order to attain commensurism or coincidence. In the absence of very strong substrate-overlayer interactions, molecular overlays must achieve epitaxy by coincidence as the overlayer will tend to retain its native form, or be only slightly reconstructed, because the energetic penalty of severe reconstruction will be larger than the benefit of achieving commensurism. Conversely, in the presence of very strong overlayer-substrate interactions the local non-commensurism of molecules contained within the non-primitive supercell would be highly unfavorable and the overlayer will tend to a commensurate form.

The competition between intra and interlayer interactions also can be described in terms of the elasticity of the overlayer and the overlayer-substrate interface.<sup>10</sup> Reconstruction of an overlayer accompanying the formation of commensurate or coincident lattices is tantamount to introducing intralayer strain, described by the difference between the positions of the molecules in the reconstructed and native forms. This strain will impart an intralayer stress that, for a sufficiently small strain, can be described by a linear stress-strain relationship. The stress and strain in a three-dimensional solid are second rank tensors and can be used to analyze the elastic properties of a thin film-substrate interface (Figure 7). Stresses between the overlayer and substrate due to molecules located on non-commensurate positions ( $\sigma_{x\text{ inter}}$ ,  $\sigma_{y\text{ inter}}$ , and  $\sigma_z\text{ inter}$ ) create interfacial forces which drive reconstruction of the overlayer toward commensurate forms. These stresses are opposed by intralayer stresses ( $\sigma_x\text{ intra}$  and  $\sigma_y\text{ intra}$ ) accompanying reconstruction of the native overlayer structure. If only the purely extensional components of the strain tensor, parallel to the film interface and directed along x and y ( $\varepsilon_x$  and  $\varepsilon_y$ ), are considered the stress-strain relations for the intralayer components are given by eqs. (19) and (20).

The intralayer elastic constants  $c_{xx\text{ intra}}$  and  $c_{yy\text{ intra}}$  represent the "stiffness" of the overlayer, that is, its resistance to reconstruction from its preferred or native structure. The elastic constants can be determined by calculation of the second derivative of the corresponding potential functions, the second derivative

simply being the radius of curvature of the potential well,  $\kappa = d^2V/dr^2$ . The larger the value of  $\kappa$ , the larger the stiffness constant and the greater the opposition to perturbations from the minimum energy configuration. The radius of curvature of the potential generally will scale with its depth, implying that larger interaction energies generally will lead to larger elastic constants.

[Figure 7]

The stress component oriented normal to the substrate interface  $\sigma_z$  is related to the strain  $\epsilon_z$ , which describes changes in the overlayer-substrate separation along the  $z$ -axis, by the elastic constant  $c_{22}^{\text{inter}}$  (eq. 21). Strain at the overlayer-substrate interface along the  $x$ -axis, such as that resulting from molecules sitting on locally non-commensurate positions in coincident overlayers, will result in a stress along  $x$  and a shear stress along  $z$  according to eqs. (22) and (23).

$$\sigma_z^{\text{inter}} = c_{zz}^{\text{inter}} \epsilon_z \quad (21)$$

$$\sigma_x^{\text{inter}} = c_{xx}^{\text{inter}} \epsilon_x \quad (22)$$

$$\sigma_z^{\text{inter}} = c_{xz}^{\text{inter}} \epsilon_x \quad (23)$$

Small overlayer-substrate elastic constants and large intralayer elastic constants will conspire to favor coincident overlayers, as the interfacial stress associated with molecules on non-ideal positions will be smaller than the intralayer stress that would accompany reconstruction of the overlayer from its native form to a reconstructed overlayer that is commensurate with the substrate. The competition between interfacial and intralayer interactions and stiffness is evident from comparison of the PTCDA/Cu(100), PTCDA/HOPG, and PTCDA/MoS<sub>2</sub> systems. A highly

reconstructed commensurate overlayer is observed on Cu(100), while on HOPG and MoS<sub>2</sub> coincident overlayers are observed with a structure comparable to those in the bulk crystal. The formation of a commensurate structure on Cu(100) suggests strong chemisorption on the high-energy Cu(100) surface. In contrast, the interfacial interactions, and the corresponding interfacial stresses, are expected to be smaller on the lower energy HOPG and MoS<sub>2</sub> surfaces, enabling formation of coincident lattices for which intralayer forces dominate the overlayer structure.

Recent studies in our laboratory have demonstrated that molecular overlayers with structures mimicking layers in bulk crystals of conducting charge-transfer salts can be grown epitaxially on ordered substrates such as HOPG. Among the systems we have investigated, three are illustrative of the influence of overlayer-substrate energetics: (ET)<sub>2</sub>I<sub>3</sub>||HOPG, (Pe)<sub>2</sub>ClO<sub>4</sub>||HOPG, and (TTF)(TCNQ)||Au(111) (Figure 8). The azimuthal orientations of the overlayers for (ET)<sub>2</sub>I<sub>3</sub>||HOPG and (Pe)<sub>2</sub>ClO<sub>4</sub>||HOPG were established directly by atomic force microscopy during electrochemical growth of these monolayers in solution.<sup>34,36,37</sup> This was accomplished by obtaining lattice images of the overlayer and comparing their orientation to the bare substrate lattice in regions either adjacent to the overlayer or beneath the overlayer (produced after mechanical etching of the overlayer with the AFM tip). The overlayer structures, all of which were coincident with the HOPG substrate, reflect the balance between interfacial and intralayer elasticity (Table 2). In the case of (ET)<sub>2</sub>I<sub>3</sub> a coincident overlayer was observed whose lattice constants were identical, within experimental error, to those of the molecular (001) layers in the bulk crystal of β-(ET)<sub>2</sub>I<sub>3</sub>. Analysis of V/V<sub>0</sub> based on the bulk crystal lattice parameters for β-(ET)<sub>2</sub>I<sub>3</sub> for this overlayer indicated coincidence at  $\theta = 19^\circ$ , in near agreement with the experimentally observed value of  $\theta = 18^\circ$ .

[Table 2]

**Table 2:** The azimuthal angle, lattice constants, adsorption energies, variation of adsorption energies with respect to overlayer position, for molecular films based on charge-transfer salts. The experimental values of  $\theta$ ,  $b_1$ ,  $b_2$ , and  $\beta$  were determined by either AFM or STM.

Overlayer	$\theta$ (deg)	$b_1$ (Å)	$b_2$ (Å)	$\beta$ (deg)	$c_{xx}$ (kcal mol <sup>-1</sup> Å <sup>-2</sup> )	$c_{yy}$ (kcal mol <sup>-1</sup> Å <sup>-2</sup> )	$c_{xz}$ (kcal mol <sup>-1</sup> Å <sup>-2</sup> )	$c_{zx}$ (kcal mol <sup>-1</sup> Å <sup>-2</sup> )
<b>(Pe)<sub>2</sub>ClO<sub>4</sub>/HOPG</b>								
Calculated <sup>a</sup>	9	13.2	19.2	90	6.6	5.4	167	1.74
AFM	15	10.9±0.6	18.1±0.3	87				
Bulk Crystal <sup>c</sup>	b	13.1	14.1	90				
<b>(TTF)(TCNQ)Au(111)</b>								
Calculated <sup>a</sup>	27	12.7	18.4	104	13.5	6.5	27.9	0.71
STM	d	11.0±0.3	16.5±0.4	104				
Bulk Crystal <sup>c</sup>	b	12.3	18.5	104				
<b>(001) β-(ET)<sub>2</sub>I<sub>y</sub>/HOPG</b>								
Calculated <sup>a</sup>	19	6.67	9.09	110	80.2	36	43.5	0.61
AFM	18 <sup>f</sup>	6.25±0.4	8.5±0.4	108				
Bulk Crystal (001 layer)	18	6.61	9.1	110				
<b>(001) β-(ET)<sub>2</sub>I<sub>y</sub>/HOPG</b>								
Calculated <sup>a</sup>	17	6.65	18.6	83	36	5	192	2.96
AFM	15	7.2±0.4	17.3±0.8	83				
Bulk Crystal (001) layer	b	6.67	18.4	82				

<sup>a</sup>The values of  $\theta$  were calculated from analysis of  $V/V_0$  using the lattice constants  $b_1$ ,  $b_2$  and  $\beta$  of the energy minimized overlayer structure, as determined with the Universal Force Field. <sup>b</sup>No epitaxial match indicated by analysis of  $V/V_0$ . <sup>c</sup>The bulk lattice constants actually are those reported for (Pe)<sub>2</sub>Pf<sub>6</sub> (reference 3). <sup>d</sup>Azimuthal orientation could not be determined experimentally. <sup>e</sup>Bulk crystal structure reported in reference 39. <sup>f</sup>AFM measurements indicated  $\theta$  values ranging from 10° - 19°, which may be due to orientational disorder with some contribution from experimental error. However, determination of the orientation of microcrystals on the HOPG by AFM, which is more reliable, indicated that  $\theta = 18^\circ$ .

[Figure 8]

This coincident  $\beta$ -(ET)<sub>2</sub>I<sub>3</sub> overlayer is described by a  $1 \times 3$  non-primitive commensurate supercell which contains molecules within its perimeter that reside on non-commensurate lattice positions. The non-ideality of these positions represent local strains but calculations indicate that the interfacial stresses resulting from these strains are likely to be small. The calculated adsorption energy for a (001)  $\beta$ -(ET)<sub>2</sub>I<sub>3</sub> unit cell on HOPG was 15.1 kcal mol<sup>-1</sup> (at  $\theta = 0^\circ$ ) and the dependence of potential V on translation and azimuthal rotation was rather shallow, varying only by 0.2 kcal mol<sup>-1</sup>. This is tantamount to small interfacial elastic constants  $c_{xx}$  and  $c_{xz}$ , and consequently, the stresses  $\sigma_x$  and  $\sigma_z$  associated with placing molecules on non-commensurate interfacial values (Table 1). This signals that the energetic penalty resulting from reconstruction of the coincident overlayer to a commensurate overlayer is greater than the energetic penalty associated with the non-commensurate overlayer sites in the coincident structure. The observations of an unreconstructed  $\beta$ -(ET)<sub>2</sub>I<sub>3</sub> (001) overlayer can be attributed to strong intralayer interactions and large elastic constants associated with strong  $\pi$ - $\pi$  interactions along the ET stacks and in plane S-S interactions between ET molecules in a direction perpendicular to these stacks, but weak van der Waals interactions between (001) layers which serve to minimize the surface energy of this plane. Indeed, the energy minimized structure of the (001) layers was essentially identical to that observed in the bulk crystal. The ability of this native form to achieve coincidence provides sufficient stabilization of the overlayer so that energetically unfavorable reconstruction to a commensurate overlayer is obviated. It is worth noting that analysis of  $V/V_0$  for (ET)<sub>2</sub>I<sub>3</sub> molecular layers in the numerous polymorphs known for this composition or composition variants<sup>37</sup> did not reveal any coincident relationships with HOPG. These polymorphs contain similar layer structures, also with large intralayer elasticities, suggesting that the energetic penalty associated with reconstruction to coincident or commensurate structures is too large for these to be formed.

In contrast to the (001)  $\beta$ -(ET)<sub>2</sub>I<sub>3</sub> overlayer, analysis of V/V<sub>0</sub> for molecular (Pe)<sub>2</sub>ClO<sub>4</sub><sup>38</sup> and (TTF)(TCNQ)<sup>39</sup> layers did not identify any native layers which were epitaxial with HOPG and Au(111) substrates, respectively.<sup>40</sup> Nevertheless, AFM and STM revealed the formation of molecularly thick overlayers (ca. 4 Å) with lattice constants differing from those of the bulk layers or energy minimized forms of these layers. Analysis of V/V<sub>0</sub> based on the AFM and STM lattice constants indicated that these overlayers were coincident at azimuthal angles of  $\theta = 90^\circ$  and  $\theta = 270^\circ$  for (Pe)<sub>2</sub>ClO<sub>4</sub>/HOPG and (TTF)(TCNQ)/Au(111), respectively. In the case of (Pe)<sub>2</sub>ClO<sub>4</sub>/HOPG the calculated azimuthal angle was identical, within experimental error, to that measured by AFM. Experimental difficulties related to the stability of the (TTF)(TCNQ) overlayers on Au(111) during scanning with the STM have thus far prevented reliable determination of the azimuthal angle for this system. However, we presume that it is coincidence at  $\theta = 270^\circ$  that stabilizes this overlayer. The 4 Å thickness of the overlayers in each case suggested that the molecular planes were parallel to the substrates, resembling the (100) plane in (Pe)<sub>2</sub>ClO<sub>4</sub> and the (010) plane in (TTF)(TCNQ). However, these overlayers are substantially reconstructed from their "native" forms given the difference between the crystallographic constants and those determined by AFM and STM (Figure 8). Furthermore, the lattice constants of the energy minimized layer structures also differed substantially from their native bulk forms. The intralayer interactions are primarily van der Waals in nature with additional contributions from ion-ion interactions (the latter were disregarded in our calculations because parallel studies have indicated that their contribution was minimal due to their long range nature). The calculated values given in Table 2 indicate that the intralayer elastic constants of the (Pe)<sub>2</sub>ClO<sub>4</sub> overlayer are substantially smaller than those of the (001)  $\beta$ -(ET)<sub>2</sub>I<sub>3</sub> overlayer, consistent with weaker intralayer interactions and reduced overlayer stiffness. Conversely, the calculated adsorption energy of a unit cell of (Pe)<sub>2</sub>ClO<sub>4</sub> on HOPG is -92.4 kcal mol<sup>-1</sup> (at  $\theta = 0^\circ$ ) and the variation in this energy is 0.8 kcal mol<sup>-1</sup>, both substantially higher than that calculated for the (001)  $\beta$ -(ET)<sub>2</sub>I<sub>3</sub> overlayer. This is due to stronger interfacial interactions associated with the Pe molecular planes lying parallel to the HOPG surface, which results in a

greater dispersive interaction per molecule. Consequently, the interfacial elastic constants are substantially higher and the energetic benefit of coincident epitaxy outweighs the penalty associated with the reconstruction required to achieve coincidence. However, the absence of a completely commensurate overlayer structure indicates that such a severe reconstruction is energetically prohibitive. Similar arguments support the observation of a (TTF)(TCNQ) layer which is substantially reconstructed from its native (010) layer structure. We surmise that strong gold-sulfur interactions play an important role in the observed orientation and in the reconstruction to a lattice which is compressed compared to the bulk layer structure.

The delicate balance of these factors can be illustrated further by our observation of a second orientation of (ET)<sub>2</sub>I<sub>3</sub> on HOPG for which the overlayer structure resembles a reconstructed (011) layer from  $\beta$ -(ET)<sub>2</sub>I<sub>3</sub> (recent experiments suggest that this layer may actually be the precursor of the (001) orientation). This coincident overlayer is described by flat-lying molecules in which intralayer S-S heteroatom interactions are present but the  $\pi-\pi$  overlap is absent, which results in smaller intralayer interactions and elastic constants compared to the (001) orientation. The calculated absorption energy for this orientation was -40 kcal mol<sup>-1</sup> (at  $\theta = 0^\circ$ ) and the spread of adsorption energies was 0.8 kcal mol<sup>-1</sup>, leading to larger interfacial elastic constants than those observed for the (001) orientation. These factors favor reconstruction of the native layer structure to a form that can achieve coincidence, but not commensurism.

These observations reveal the factors controlling the mode of overlayer growth. The most favorable growth mode will be that in which coincidence is achieved by a unreconstructed (or very slightly reconstructed) molecular layer with strong intralayer interactions. In this configuration the overlayer structure is at or near its energy minimum, the surface energy is minimized because the strongest interactions are within the plane of the overlayer, the intralayer stiffness exceeds that of the overlayer-substrate interface and epitaxial stabilization can be achieved by coincidence. If epitaxy with such an overlayer is not possible, its large intralayer elastic constant will inhibit the reconstruction required to achieve coincidence or commensurism. Under this condition the system will likely favor the growth of epitaxial overlayers whose structures resemble alternative bulk

crystal planes with smaller intralayer interactions and elastic constants. This reduces the energetic penalty of overlayer reconstruction necessary to achieve epitaxy by either coincidence or commensurism. However, this can lead to growth orientations in which the strongest intermolecular interactions are perpendicular to the overlayer, as is the case for (Pe)<sub>2</sub>ClO<sub>4</sub>||HOPG, (011)  $\beta$ -(ET)<sub>2</sub>||HOPG, and (TTF)(TCNQ)||Au(111). Under this condition, the elastic constants defining the interface between layers are expected to be large. Because the structure of a reconstructed primary overlayer differs from its bulk native form, this can lead to significant stresses during growth of multilayer than films from these primary overlayers.

## CONCLUSIONS

We have demonstrated that a simple analytical function can be used to analyze the epitaxy between molecular overlayers and rigid ordered substrates. This method predicts whether an overlayer is commensurate or coincident, and predicts the azimuthal angles required for these conditions. Comparison with total potential energy calculations reveals that the dependence of overlayer-substrate potential upon azimuthal angle is reproduced by V/V<sub>0</sub>. The validity of the analytical method is corroborated further by the good agreement of V/V<sub>0</sub> minima with the azimuthal orientations for numerous overlayer structures observed experimentally. The advantage of this approach is that the computation is independent of overlayer size, which enables rapid analysis for large basis sets and large overlayers. This is crucial for identifying coincident lattices as potential energy calculations, which are necessarily limited to small numbers of overlayer unit cells due to their computational intensiveness, can yield shallow minima that incorrectly suggest incommensurism. The type of epitaxy and optimum azimuthal angle can be determined in seconds on a low-cost CPU, enabling convenient searching for possible reconstructed overlayer configurations in which the lattice parameters  $a_1$ ,  $b_2$  and  $\beta$  are bracketed around the native overlayer values so that slight epitaxy-driven reconstructions can be surmised. This method can be used to determine the likelihood of epitaxy of different polymorphic forms of an overlayer if these polymorph structures are known, providing some predictability of the overlayer structure. If these

overlayers serve as nuclei for multilayers or bulk crystals, this can serve as a convenient approach to selecting substrates for selective crystallization of thin film structures or crystals that tend to exhibit polymorphism. When combined with analysis of the elastic constants for a given overlayer-substrate configuration this provides a convenient approach for the *a priori* design of heteroepitaxial molecular films and substrates for the growth of multilayer films and bulk crystals.

**ACKNOWLEDGEMENTS.** The authors gratefully acknowledge Mr. Christopher M. Yip for writing the Windows™ version of EpicCalc®. Financial support was provided by the Office of Naval Research and the Center for Interfacial Engineering, an NSF/ERC.

## REFERENCES

- (a) A. Aviram and M. Rainer, *Chem. Phys. Lett.* **29**, 277 (1974). (b) *Molecular Electronic Devices*, F. Carter, Ed. (Marcel Dekker, New York, 1982). (c) *Molecular Electronics*, G. Ashwell, Ed. (John Wiley and Sons, New York, 1992).
- (a) M. Matsunoto, T. Nakamura, E. Manda, and Y. Kawabata, *Thin Solid Films* **160**, 61 (1988). (b) K. Naito, A. Miura, and M. Azuma, *J. Am. Chem. Soc.* **113**, 6386 (1991).
- (c) A. Dhindsa, Y.-P. Song, J. Badyal, M. Bryce, Y. Lvov, and M. Petty, *J. Chem. Mater.* **4**, 724 (1992). (d) C.M. Yip and M.D. Ward, *Langmuir* **10**, 549 (1994).
- (a) G. Cao, H.-G. Hong, and T. E. Mallouk, *Acc. Chem. Res.* **25**, 420 (1992). (b) M. E. Thompson, *Chem. Mater.* **6**, 1168 (1994).
- S. Yitzchak, S. B. Roscoe, A. K. Kakkar, D. S. Allan, T. J. Marks, Z. Xu, T. Zhang, W. Lin, G. K. Wong, *J. Phys. Chem.* **97**, 6958 (1993).
- (a) A. C. Hillier, J. B. Marson, and M. D. Ward, *Chem. Mater.* **6**, 2222 (1994). (b) Ph. D. Thesis, A. C. Hillier, University of Minnesota, 1995.
- (a) G.E. Collins, K.W. Nebeary, C. England, L. Chau, P.A. Lee, B. Parkinson, Q. Fernando, and N.R. Armstrong, *J. Vac. Sci. Technol. A* **10**, 2902 (1992). (b) C.

- Ludwig, B., Gompf, W., Platz, J., Peterson, W., Eisenmenger, M., Mobus, U., Zimmerman, and N. Karl, *Z. Phys. B* **86**, 397 (1992). (c) C. Ludwig, B. Gompf, J. Peterson, R. Strohmaier, and W. Eisenmenger, *Z. Phys. B* **93**, 365 (1993). (d) N.R. Armstrong, K.W. Nebesny, G.E. Collins, L.-K. Chau, P.A. Lee, C.D. England, D. Diehl, M. Douskey, and B. Parkinson, *Thin Solid Films* **216**, 90 (1992). (e) K.W. Nebesny, G.E. Collins, P.A. Lee, L.-K. Chau, J. Danziger, E. Osburn, and N.R. Armstrong, *Chem. Mater.* **3**, 829 (1991).
- <sup>7</sup> *Epitaxial Growth*, J. Matthews, Ed. (Academic Press, New York, 1975).
- <sup>8</sup> (a) S.R. Forrest and Y. Zhang, *Phys. Rev. B* **49**, 11297 (1994). (b) Y. Zhang and S.R. Forrest, *Phys. Rev. Lett.* **71**, 2765 (1993).
- <sup>9</sup> R.P. Searinge, in *Electron Crystallography of Organic Molecules*, J. R. Fryer, D.L. Dorset, Eds., Kluwer, Boston, 1991, p85.
- <sup>10</sup> J. Perlstein, *J. Amer. Chem. Soc.* **116**, 11420 (1994).
- <sup>11</sup> A. Hoshino, S. Isoda, H. Kurata, and T. Kobayashi, *J. Appl. Phys.* **76**, 4113 (1994).
- <sup>12</sup> (a) K. Bender, I. Hennig, D. Schweitzer, K. Dietz, H. Endres, and H. Keller, *Mol. Cryst. Liq. Cryst.* **108**, 359 (1984). (b) T.J. Emge, P. Leung, and M. Beno, *Mol. Cryst. Liq. Cryst.* **132**, 363 (1986).
- <sup>13</sup> A. C. Hillier and M. D. Ward, *Science* **268**, 1261 (1994).
- <sup>14</sup> A. C. Hillier, P. W. Carter, and M. D. Ward, *J. Amer. Chem. Soc.* **116**, 944 (1994).
- <sup>15</sup> E.S. Pysh and N.C. Yang, *J. Am. Chem. Soc.* **85**, 2124 (1963).
- <sup>16</sup> D. Roseinsky and P. Kathirgamanathan, *J. Chem. Soc. Perkin Trans. II* 135 (1985).
- <sup>17</sup> A.K. Rappe, C.J. Casewit, K.S. Colwell, W.A. Goddard III and W.M. Skiff, *J. Am. Chem. Soc.* **114**, 10024 (1992).
- <sup>18</sup> H. Reiss, *J. Appl. Phys.* **39**, 5045 (1968).
- <sup>19</sup> (a) F.C. Frank and J.H. van der Merwe, *Proc. Roy. Soc. A* **198**, 205 (1949). (b) J.H. van der Merwe, *J. Appl. Phys.* **41**, 4725 (1970).
- <sup>20</sup> A.I. Kitaigorodsky, *Molecular Crystals and Molecules*, (Academic Press, New York, 1973).
- <sup>21</sup> MM2/MMP2: (a) N.L. Allinger, *J. Am. Chem. Soc.* **99**, 8127 (1977). (b) J.T. Sprague, J.C. Tai, Y. Yuh, and N.L. Allinger, *J. Comput. Chem.* **8**, 581 (1987). AMBER: (c) S.J. Weiner, P.A. Kollman, D.A. Case, U.C. Singh, C. Ghio, G. Alagona, S. Profeta Jr., and P. Weiner, *J. Am. Chem. Soc.* **106**, 765 (1984). (d) S.J. Weiner, P.A. Kollmann, D.T. Nguyen, and D.A. Case, *J. Comput. Chem.* **7**, 230 (1986). CHARMM: (e) B.R. Brooks, R.E. Brucoleri, B.D. Olafson, D.J. States, S. Swaminathan, and M. Karplus, *J. Comput. Chem.* **4**, 187 (1983). (f) L. Nilsson, and M. Karplus, *J. Comput. Chem.* **7**, 591 (1986).
- <sup>22</sup> UFF: A. Rappe, C. Casewit, K. Colwell, W. Skiff, J. Am. Chem. Soc. **114**, 10024 (1992).
- <sup>23</sup> DREIDING: S. Mayo, B. Olafson, and W. Goddard, *J. Phys. Chem.* **94**, 8897 (1990).
- <sup>24</sup> J.H. van der Merwe, *Phil. Mag. A* **45**, 127 (1982).
- <sup>25</sup> (a) F.C. Frank, *J.H. van der Merwe*, *Proc. Roy. Soc. A* **198**, 205 (1949). (b) F.C. Frank and J.H. van der Merwe, *Proc. Roy. Soc. A* **198**, 216 (1949). (c) J.H. van der Merwe, *Phil. Mag. A* **45**, 145 (1982). (d) J.H. van der Merwe, *Phil. Mag. A* **45**, 159 (1982). (e) J.H. van der Merwe, *J. Appl. Phys.* **41**, 4725 (1976). (f) H. Reiss, *J. Appl. Phys.* **39**, 5045 (1968). (g) A.D. Novaco and J.P. McTague, *Phys. Rev. Lett.* **38**, 1286 (1977). (h) A.D. Novaco and J.P. McTague, *Phys. Rev. B* **19**, 5299 (1979).
- <sup>26</sup> (a) M.L. Anderson, V.S. Williams, T.J. Schuellein, G.E. Collins, C.D. England, L.-K. Chau, P.A. Lee, K.W. Nebesny, and N.R. Armstrong, *Surf. Sci.* **307-309**, 551 (1994). (b) C. Ludwig, B. Gompf, J. Peterson, R. Strohmaier, and W. Eisenmenger, *Z. Phys. B* **93**, 365 (1993).
- <sup>27</sup> (a) E. Haskal, F. So, P. Burrows, and S. Forest, *Appl. Phys. Lett.* **60**, 3223 (1992). (b) S.R. Forrest, P.E. Burrows, E.I. Haskal, and Y. Zhang, *Mat. Res. Soc. Symp. Proc.* **328**

- (1994). (c) Y. Zhang and S.R. Forrest, *Phys. Rev. Lett.* **71**, 2765 (1993). (d) S.R. Forrest and Y. Zhang, *Phys. Rev. B* **49**, 11297 (1994). (e) P.E. Burrows, Y. Zhang, I. Haskal, and S.R. Forrest, *Appl. Phys. Lett.* **61**, 2417 (1992).
- 28 (a) C. Ludwig, B. Gompf, W. Flatz, J. Peterson, W. Eisenmenger, M. Mobus, U. Zinnermann, and N. Karl, *Z. Phys. B* **86**, 397 (1992). (b) C. Ludwig, B. Gompf, J. Peterson, R. Strohmaier, and W. Eisenmenger, *Z. Phys. B* **93**, 365 (1993).
- 29 T.J. Schuerlein and N.R. Armstrong, *J. Vac. Sci. Technol. A* **12**, 1992 (1994).
- 30 C. Ludwig, R. Strohmaier, J. Peterson, B. Gompf, and W. Eisenmenger, *J. Vac. Sci. Technol. B* **12**, 1963 (1994).
- 31 J.C. Bucholz and G.A. Sonnajai, *J. Chem. Phys.* **66**, 573 (1977).
- 32 A.C. Hillier and M.D. Ward, manuscript in preparation.
- 33 (a) J.H. Schott and M.D. Ward, *J. Am. Chem. Soc.* **116**, 6806 (1994). (b) A.C. Hillier, J.H. Schott, and M.D. Ward, *Adv. Mater.* **7**, 409 (1995).
- 34 A.C. Hillier and M.D. Ward, manuscript in preparation.
- 35 A.C. Hillier and M.D. Ward, manuscript in preparation.
- 36 (a) P.E. Burrows, Y. Zhang, I. Haskal, and S.R. Forrest, *Appl. Phys. Lett.* **61**, 2417 (1992). (b) Y. Zhang and S.R. Forrest, *Phys. Rev. Lett.* **71**, 2765 (1993). (c) S.R. Forrest and Y. Zhang, *Phys. Rev. B* **49**, 11297 (1994).
- 37 Organic Superconductors. J. M. Williams, J. R. Ferraro, R. J. Thom, K. D. Carlson, U. Geiser, H. H. Wang, A. M. Kini and M.-H. Whangbo, *Organic Superconductors*, (Prentice Hall, Englewood Cliffs, New Jersey, 1992).
- 38 The structure of  $(Pe)_2ClO_4$  was assumed to be similar to that of  $(Pe)_2PF_6$ , which crystallizes in the  $P\bar{2}/m$  space group with  $a = 13.04 \text{ \AA}$ ,  $b = 14.12 \text{ \AA}$ ,  $c = 13.75 \text{ \AA}$ ,  $\beta = 110.8^\circ$ ; H. Endres, H.K. Müller, and D. Schweizer, *Acta Cryst. C* **41**, 607 (1985); H. Keller, D. Nothe, H. Prizkow, D. Wehe, and M. Werner, *Mol. Cryst. Liq. Cryst.* **62**, 181 (1980). Other polymorphs examined for epitaxy were  $(Pe)_3ClO_4$ , which crystallizes in the  $\bar{P}1$  space

**Figure Captions**

**Figure 1.** Schematic representation of a generic  $2 \times 2$  molecular overlayer on a rigid substrate. The substrate and overlayer lattices are defined by two-dimensional cells with lattice constants  $a_1$ ,  $a_2$ ,  $\alpha$  and  $b_1$ ,  $b_2$ ,  $\beta$ , respectively. The angle  $\theta$  represents the angle between the vectors  $\mathbf{a}_1$  and  $\mathbf{b}_1$ , defining the azimuthal angle of the overlayer with respect to the substrate.

**Figure 2.** (a) Schematic representation of a commensurate overlayer with  $b_1 = b_2 = 2a_1$  and  $\beta = 90^\circ$  on a primitive substrate lattice with lattice constants  $a_1 = a_2$ . (b) The dependence of the two-dimensional quasipotential  $V/V_0$  on azimuthal angle  $\theta$  for a  $20 \times 20$  overlayer for the overlayer-substrate system in (a). The minimum at  $\theta = 0$  and  $90^\circ$  corresponds to the optimum epitaxy. (c) Schematic representation of a coincident overlayer with  $b_1 = 1.6a_1$ ,  $b_2 = 1.8a_2$  and  $\beta = 146.25^\circ$ . The  $5 \times 2$  non-primitive supercell having vertices which are commensurate with the substrate is depicted. (d) The dependence of the two-dimensional quasipotential  $V/V_0$  on azimuthal angle  $\theta$  for the overlayer-substrate system in (c). The minimum at  $\theta = \pi/2$  corresponds to the optimum epitaxy.

**Figure 3.** Calculation of (a)  $V_T$ , (b)  $D(\theta)$ , and (c)  $V/V_0$  for a  $5 \times 5$  overlayer on a substrate with  $a_1 = a_2 = b_1 = b_2$ . The total potential  $V_T$  was calculated with a Lennard-Jones  $6-12$  potential using Ar atoms as the basis.

**Figure 4.** Dependence of total interaction potential  $V_T$  ( $\square$ ) and  $V/V_0$  ( $-$ ) on overlayer size for an overlayer with  $b_1 = 6.56 \text{ \AA}$ ,  $b_2 = 9.1 \text{ \AA}$ ,  $\beta = 109.8^\circ$  and a HOPG substrate with  $a_1 = 2.46 \text{ \AA}$ ,  $a_2 = 2.46 \text{ \AA}$ ,  $\alpha = 120^\circ$ . Overlayer sizes: (a)  $3 \times 3$ , (b)  $5 \times 5$ , (c)  $7 \times 7$ . In the calculation of  $V_T$ , the substrate is graphite, which contains two atoms per unit cell and the overlayer is the  $I_3$  layer of the (001) plane of b-(ET) $_2$ I $_3$ , which contains three I atoms per unit cell.

**Figure 5.** Calculated dependence of  $V/V_0$  on azimuthal angle  $\theta$  for the selected overlayer-substrate combinations depicted in Figure 6. (a) PTCDA||Cu(100), (b) CuPc||MoS<sub>2</sub>,

(c) (Pe)<sub>2</sub>ClO<sub>4</sub>||HOPG, (d) (TTF)(TCNQ)||Au(111), (e)  $\beta$ -(ET) $_2$ I $_3$  (Type I)||HOPG, (f)  $\beta$ -(ET) $_2$ I $_3$  (Type II)||HOPG. The calculations were performed using  $20 \times 20$  overlayers.

**Figure 6.** Schematic representations of overlayer orientations on substrates for selected systems in Table 1 as viewed normal to the overlayer-substrate interface. The perimeter of the primitive overlayer unit cell is depicted by a solid line. The perimeter of the non-primitive commensurate supercell for the coincident overlayers is depicted by the dashed line. (a) PTCDA||Cu(100), (b) CuPc||MoS<sub>2</sub>, (c) (Pe)<sub>2</sub>ClO<sub>4</sub>||HOPG, (d) (TTF)(TCNQ)||Au(111), (e)  $\beta$ -(ET) $_2$ I $_3$  (Type i)||HOPG, (f)  $\beta$ -(ET) $_2$ I $_3$  (Type III)||HOPG.

**Figure 7.** (a) Schematic representation of the overlayer-substrate interface for the  $\beta$ -(ET) $_2$ I $_3$  (Type I)||HOPG in which the structure of the overlayer mimicks that of the (001) molecular layers present in  $\beta$ -(ET) $_2$ I $_3$ . The stress components  $\sigma_{xx}$  and  $\sigma_{yy}$  represent purely intralayer stress resulting from extensional strain in the overlayer,  $\sigma_{xy}$  and  $\sigma_{yz}$  represents intralayer shear stress resulting from extensional strain,  $\sigma_{zz}$  represents the interfacial stress due to changes in the overlayer-substrate separation, and  $\sigma_{xz}$ ,  $\sigma_{yz}$ ,  $\sigma_{zx}$  and  $\sigma_{zy}$  are shear stress components. (b) The dependence of the total interaction potential ( $V_T$ ), stress ( $\sigma_z = dV_T/dz$ ) and elastic constant ( $C_{zz} = d^2V_T/dz^2$ ) upon overlayer-substrate separation  $z$  for (001)  $\beta$ -(ET) $_2$ I $_3$ ||HOPG for a  $1 \times 1$  overlayer. (c) Changes of  $V_T$ ,  $\sigma_z$  and  $\sigma_2$  upon translation of a  $1 \times 1$  (001)  $\beta$ -(ET) $_2$ I $_3$  overlayer on the HOPG surface along  $\mathbf{a}_1$ . The overlayer-substrate separation was fixed at  $3.4 \text{ \AA}$ . (d) Changes of  $V_T$ ,  $\sigma_x$  and  $\sigma_2$  upon rotation of the (001)  $\beta$ -(ET) $_2$ I $_3$  overlayer on the HOPG surface about a fixed axis perpendicular to the interface. The overlayer-substrate separation was fixed at  $3.4 \text{ \AA}$  and the origin of the (001)  $\beta$ -(ET) $_2$ I $_3$  unit cell was fixed at the minimum established in (b). The local minimum at  $\theta = 19^\circ$  reflects the minimum observed for large overlayer sizes (see Figure 4), whereas the deeper minimum evident at  $60^\circ$  is a false minimum resulting from the small overlayer size.

used in the calculation. (e,f) Dependence of  $V$ ,  $\sigma_x$ ,  $\sigma_y$ ,  $c_{xx}$  and  $c_{yy}$  for an isolated the (001)  $\beta$ -(ED)<sub>2</sub>I<sub>3</sub> layer. The minima of the potential wells are  $a = 6.67 \text{ \AA}$  and  $a = 9.09 \text{ \AA}$ , essentially identical to the corresponding values of  $a = 6.61 \text{ \AA}$  and  $b = 9.1 \text{ \AA}$  observed for the (001) layer in the bulk crystal. Interaction potentials were determined using a Universal Force Field.

**Figure 8.** Schematic illustration of overlayers on substrates for (a) (Pe)<sub>2</sub>ClO<sub>4</sub> on HOPG, (b) (ITF)(TCNQ) on Au(111), (c)  $\beta$ -(ET)<sub>2</sub>I<sub>3</sub> Type I on HOPG, and (d)  $\beta$ -(ED)<sub>2</sub>I<sub>3</sub> Type II on HOPG. The overlayer structures are depicted with lattice constants and azimuthal orientations ( $\theta$ ) corresponding to those observed experimentally, which agree with the values calculated from  $V/V_0$ . The actual orientation of the molecules in the overlayers are not known rigorously, and their orientations here are based on their orientations in the corresponding bulk crystals.

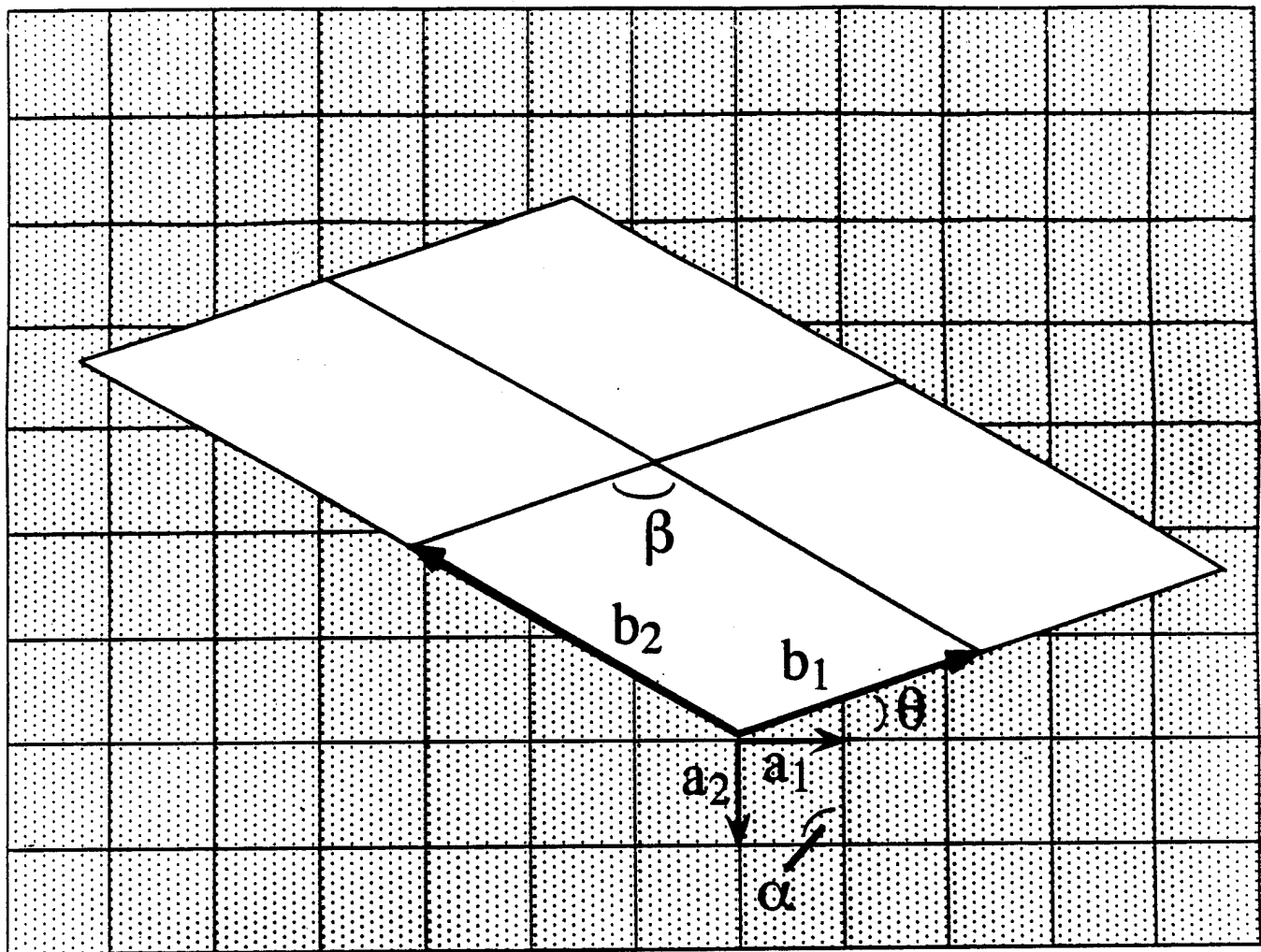
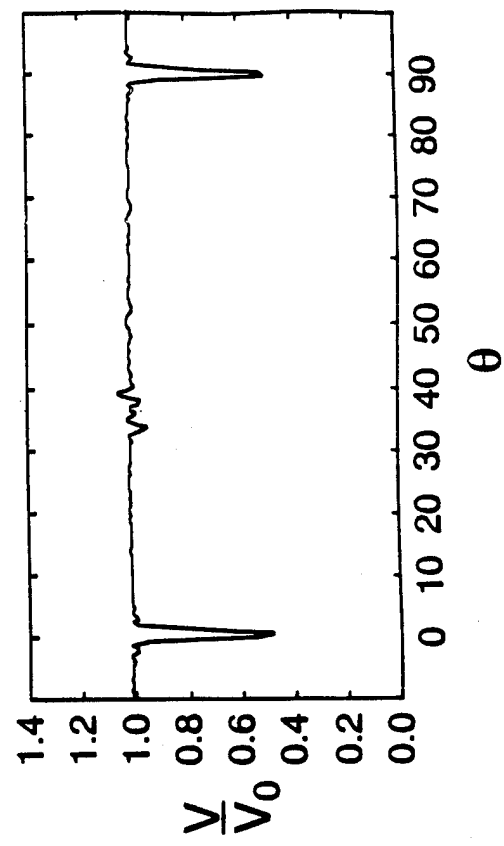
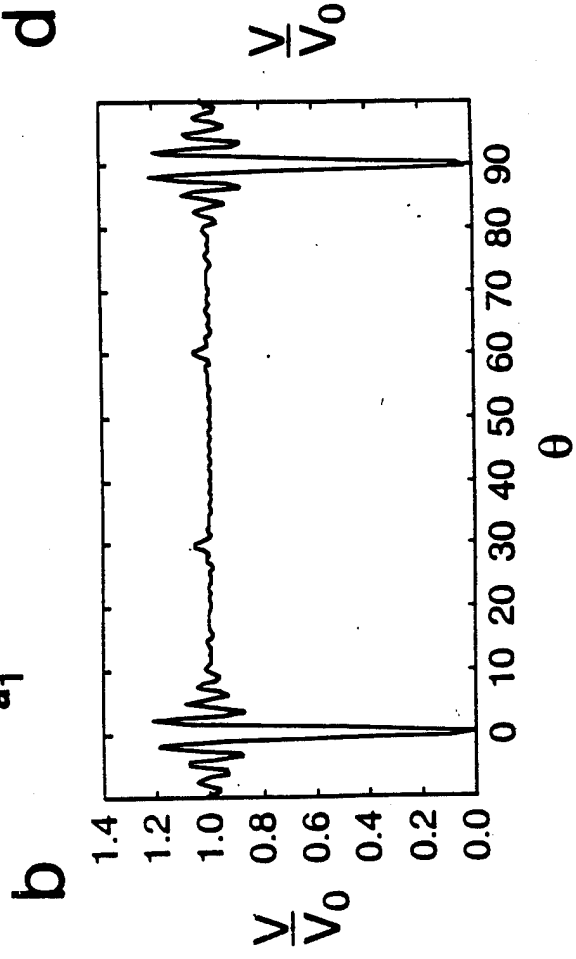
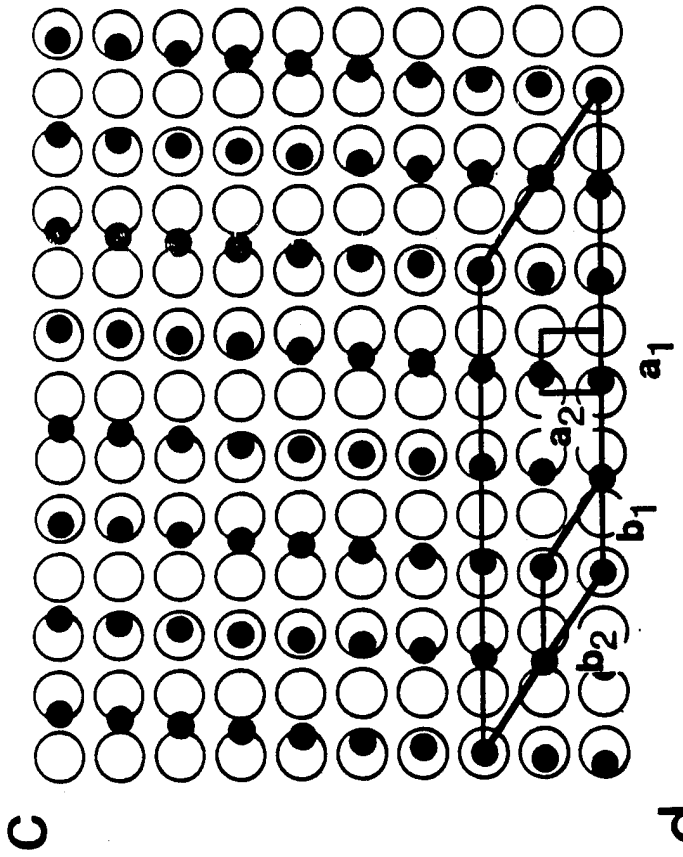
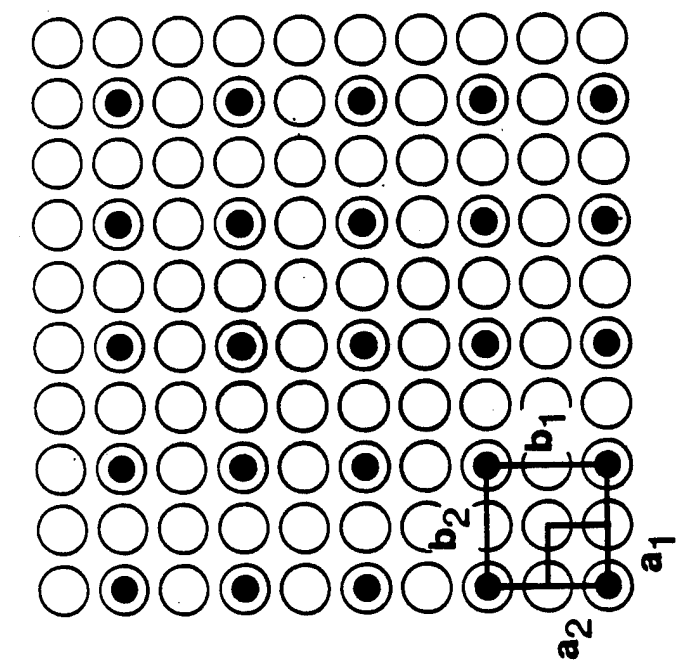
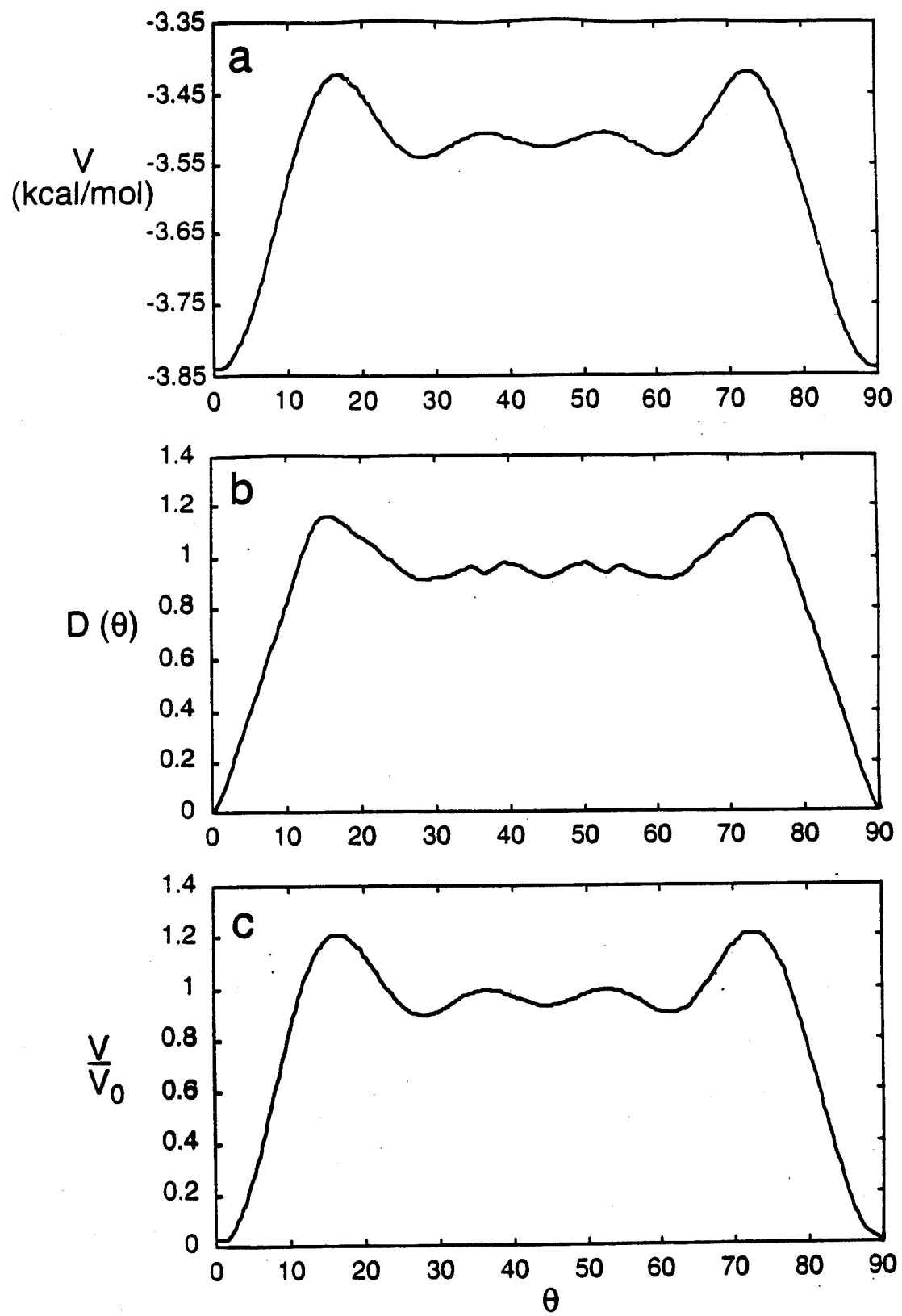
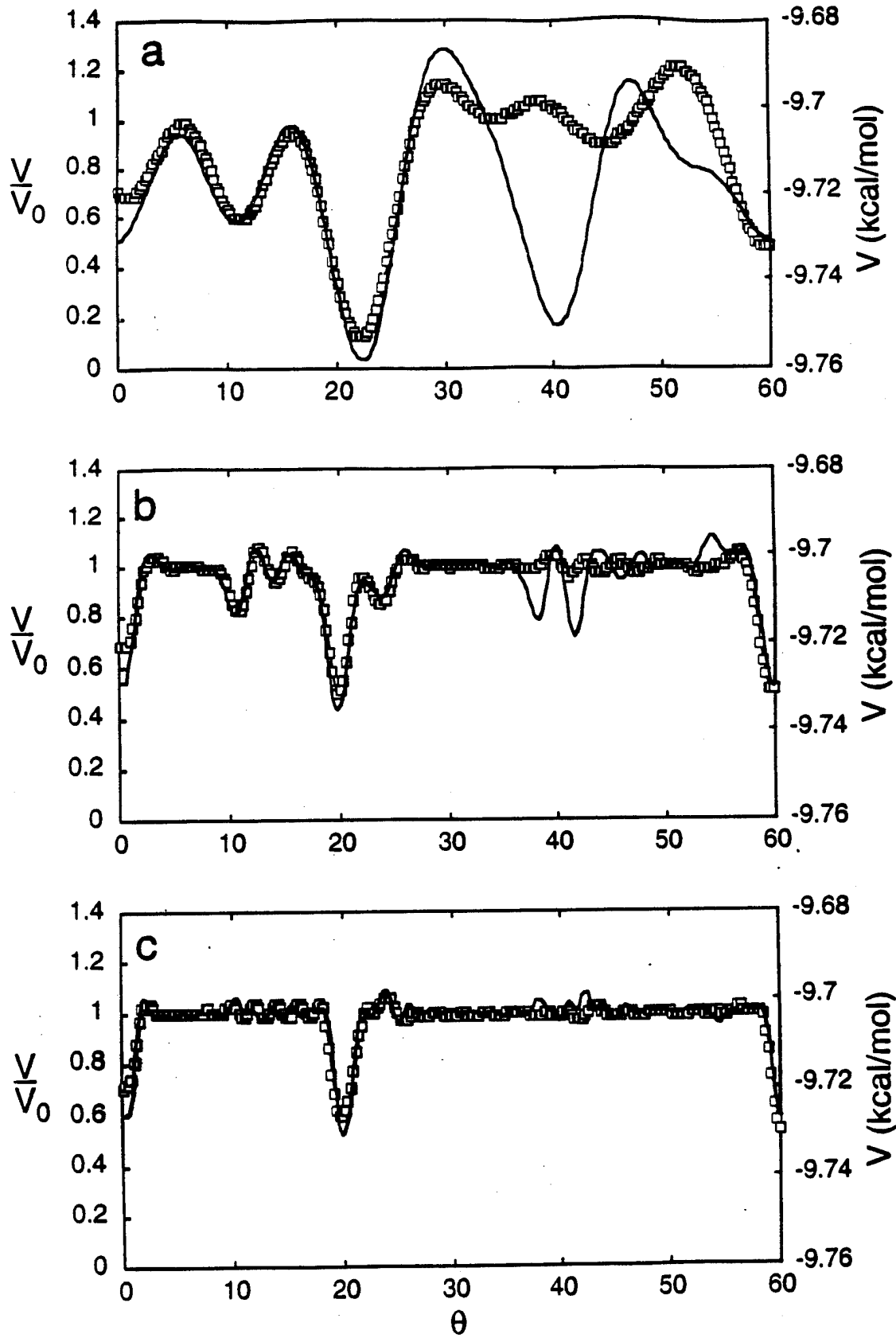
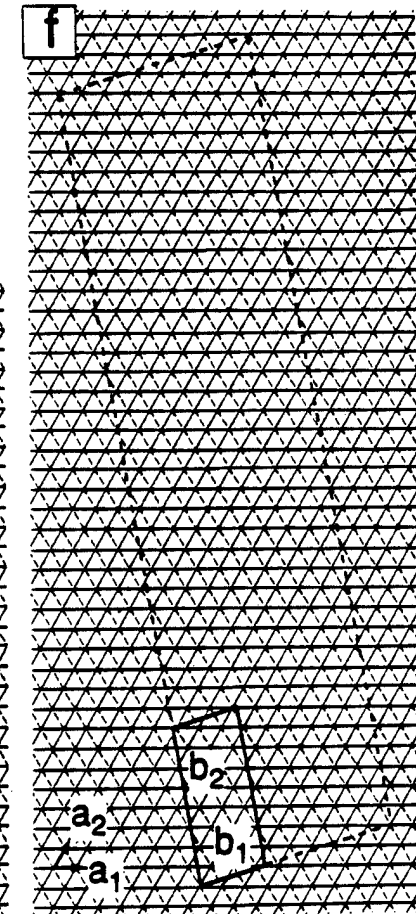
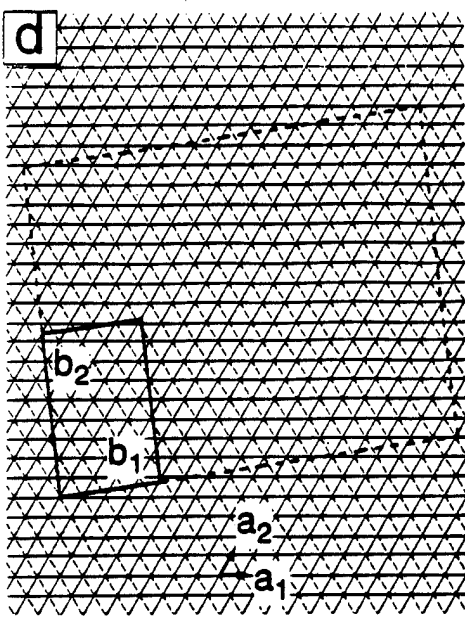
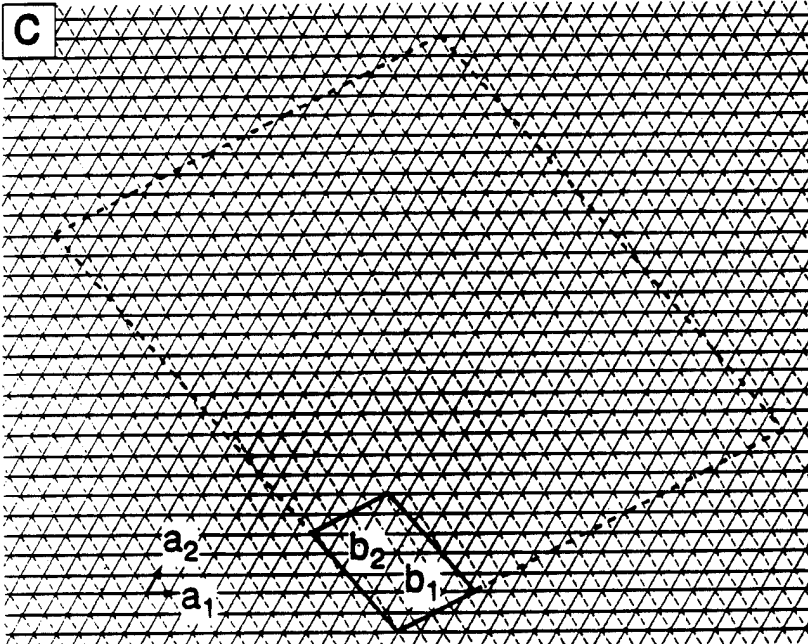
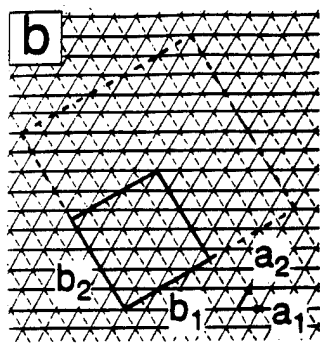
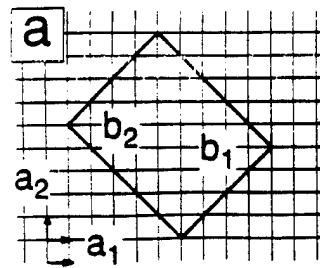


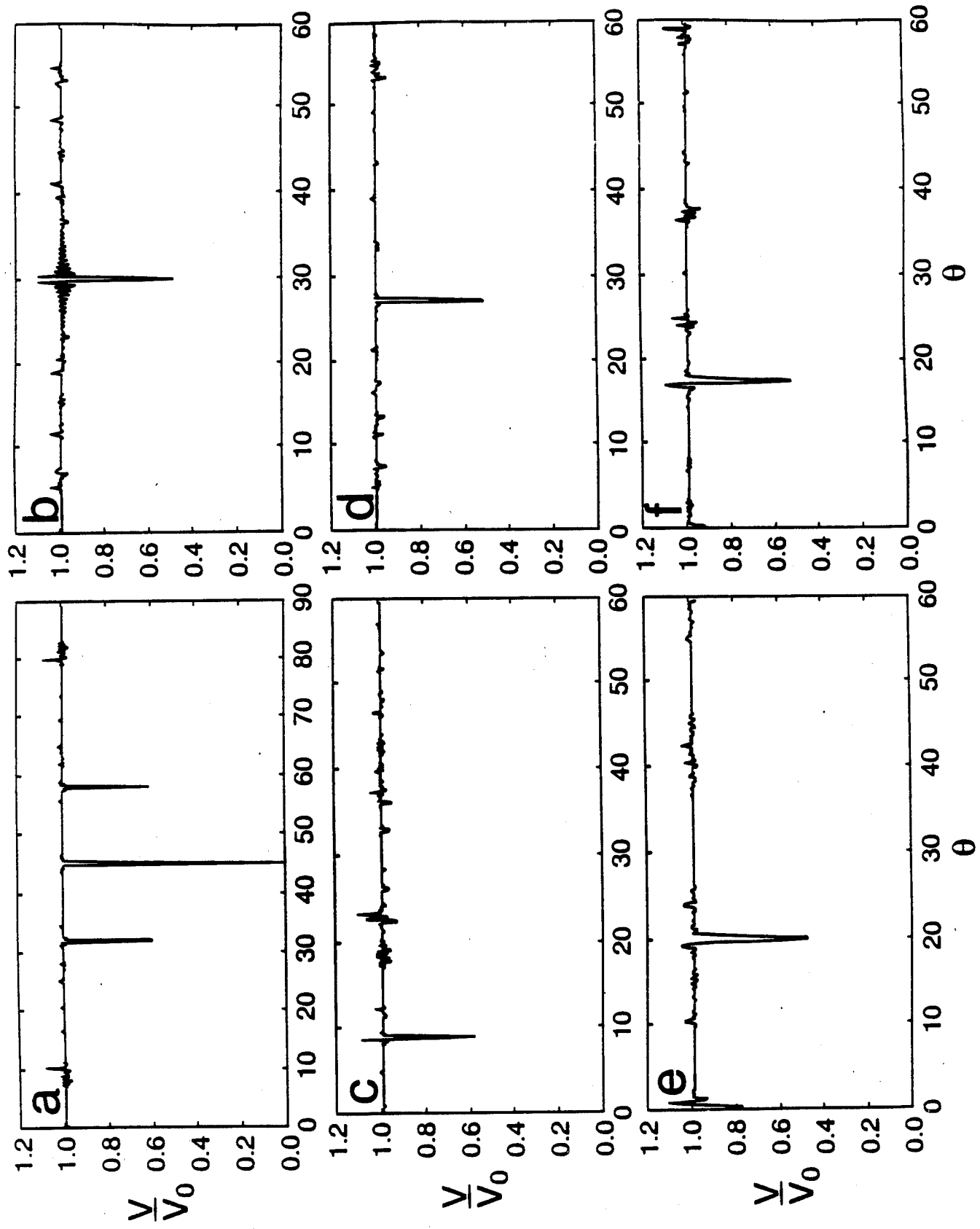
Fig 1, page 100











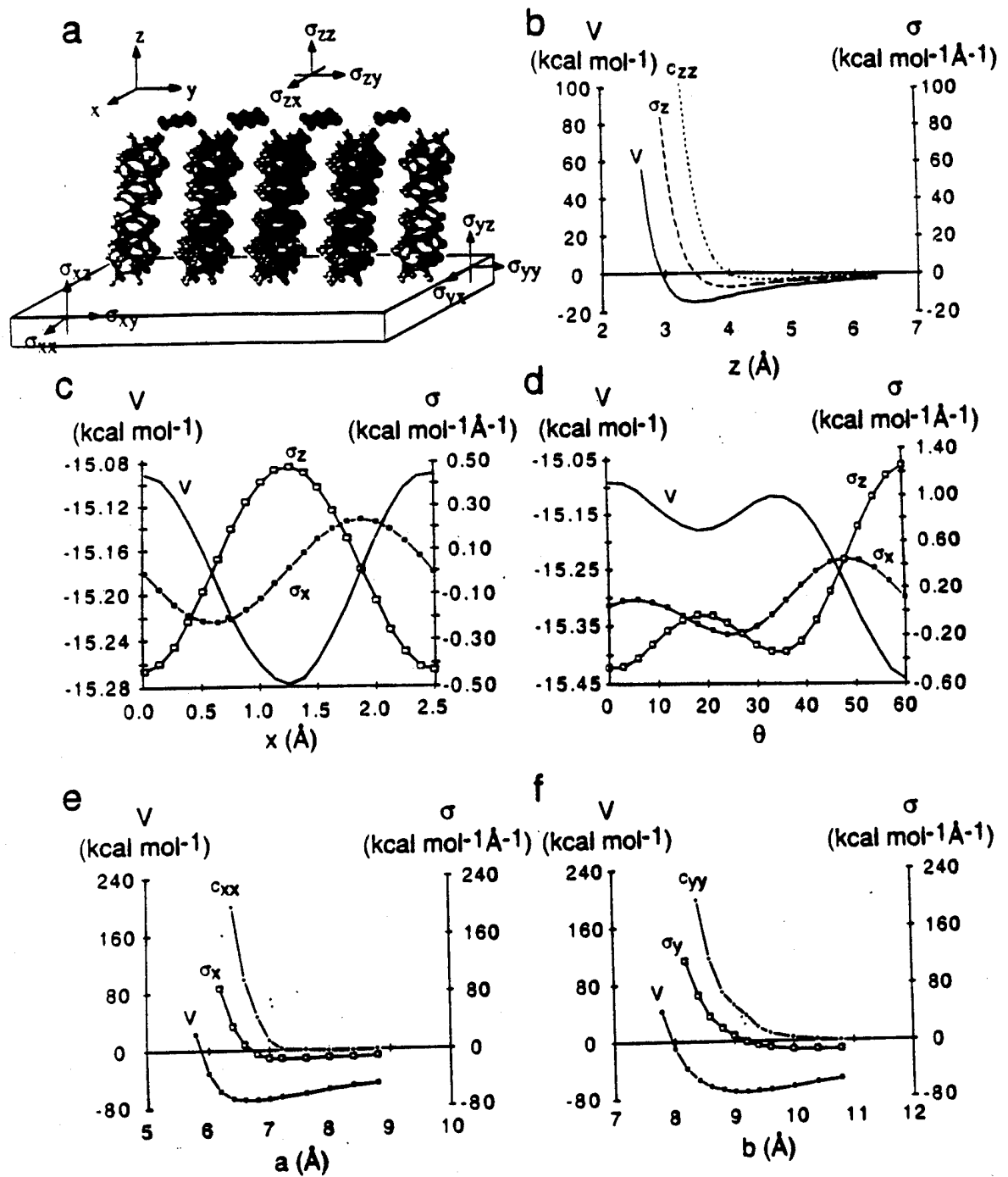


Fig 3. Miller et al.  
Phys Rev A

Fig. 2  
diamond  
graphene B

